SUPPLEMENTAL MATERIALS

Expanded Materials and Methods

Animals. All experimental protocols adhered to the guidelines of the Animal Welfare Committee of the CNIC and the Ministry of Environment and Territorial Planning of the Community of Madrid (RD 53/2013; PROEX 047/16), in compliance with European directives 86/609/EEC and 2010/63/EU. Furthermore, the procedures are reported following the ARRIVE (Animal Research: Reporting of In Vivo Experiments) guidelines[25]. The experimental groups were housed in the CNIC animal facility. The animals were kept under standard temperature and humidity conditions, with a 12-hour light-dark cycle. Food and water were provided ad libitum, both inside and outside the inverted light cabinet. Experiments were performed in 8- to 12-week-old male C57BL/6 mice and 15 months, in the case of the aged group. The following knock-in or transgenic mice were used: $Bmal^{fl/fl}MRP8^{Cre}$ or $Bmal1^{Neu}$ (mice with neutrophil-specific deficiency in Bmal1)[6,90], $Ly6G^{tdTom}$ (mice with high levels of tdTomato fluorescence in neutrophils)[33] and $Cxcr4^{fl/fl}MRP8^{Cre}$ or $Cxcr4^{Neu}$ (mice with neutrophil-specific deficiency in CXCR4). We also used $PAD4^{-/-}$ (mice with lack exons 9-10 of the peptidyl arginine deiminase type IV gene) obtained from The Jackson Laboratory (Bar Harbor, ME), and $Dnase1^{-/-}$ $Dnase1l3^{-/-}$ or $D1^{-/-}D1l3^{-/-}$ (mice without anti-dsDNA reactivity) kindly provided by Markus Napirei[91]. All transgenic mice were in the C57BL/6 background. Mice were under circadian rhythm control, as evidenced by a peak in plasma corticosterone levels shortly after the lights-off, at ZT13, by the circadian rhythmicity of metabolic and behavioral parameters (Suppl. Fig. 1) and by the time-dependent variation in leukocyte populations in peripheral blood of mice at ZT5 and ZT13 (Suppl. Fig. 2). Only male mice were used to avoid confounding effects and to reduce group numbers; we acknowledge this as a limitation, which is partly addressed by the inclusion of both sexes in the human cohort.

Experimental models of cerebral ischemia.

Animals were randomly assigned to experimental groups using a randomized fashion (coin toss). Mice were anesthetized with sevoflurane 2-3% in a mixture of 80% air/20% oxygen; body temperature was maintained at physiological levels with a heating pad during the process. In surgical procedures

a scalp incision was made, and the right temporal muscle was dissected. The area between zygomatic arch and squamous bone was thinned by a high-speed drill and cooled with saline. MCA trace was visualized with a stereomicroscope (PZMIV, World Precision Instruments, USA) and a thin bone film over MCA was lifted up.

In the *ligature model by permanent or transient middle cerebral artery occlusion* (pMCAO or tMCAO), left MCA was occluded by ligature of the trunk just before its bifurcation, between the frontal and parietal branches, with a 9-0 suture (61966, Lorca Marin) after removing the meninges in that area[92,93]. In the transient occlusion, MCA were reperfused after 75 min occlusion by removing the knot[94].

The *ferric chloride ($FeCl_3$) permanent stroke model* was performed as described[95]. A piece of Whatman filter paper strip soaked in freshly prepared ferric chloride (20%) was placed over the intact duramater in the region of the MCA for 10 min and then removed to allow the formation of a thrombus.

The *thromboembolic in situ model* was performed as described[96,97]. This model involves injecting thrombin into the MCA to create a fibrin-rich thrombus that occludes the artery. Thrombin is injected using micropipettes made from graduated capillaries, shaped to prevent bleeding during removal. The micropipette is loaded with thrombin through a pneumatic system and stored at -80°C until use. The MCA is located through a surgical procedure that involves incisions to expose the temporal bone and using a microscope to identify the artery. The micropipette is inserted into the artery lumen to inject 1 µL of thrombin, causing occlusion and a Doppler laser probe is used to measure blood flow. The occlusion is considered stable if there is a significant and sustained reduction in cerebral blood flow, measured by Doppler, and changes in vessel color. Partial or complete flow recovery in any branch is considered reperfusion.

In all types of surgeries, mice in which the MCA was exposed but not occluded served as sham-operated controls. In several experiments, naïve animals that did not undergo any type of surgery were used as control.

Infarct size determination. Infarct volume was assessed at 24h using magnetic resonance imaging (MRI) system (7T-MRI Agilent-Varian), by Nissl staining and by TTC staining (Sigma-Aldrich, T8877-50G). From Nissl staining, the slides were first digitized using the AxioScan Z1" (Zeiss®) at 40x magnification. Subsequently, 14 rostro-caudally ordered slices were measured using the NDP.view 2.7.39+ software (Hamamatsu Photonics K.K.). Infarct size in all cases was determined as described[93] and was expressed as % of injured ipsilateral hemisphere by the formula (CH-NLH/CH) X 100. The value resulting from this formula is then normalized by the edema index which is the ratio between the volume of the contralateral and ipsilateral hemisphere.

Extraction and processing of organs for flow cytometry studies. Blood was taken through cardiac puncture with 1ml syringe containing EDTA (0.5M EDTA at 0.1%) attached to a 26g needle filled with 50mL of 0.5M EDTA. Samples were lysed in 1X RBC lysis buffer (diluted from a 10X stock: KH_4Cl 1.5M, $KHCO_3$ 0.1M, EDTA-Na_2 1mM adjusted to pH 7.4) for 10min. The samples were then centrifuged at 4°C and 650 x g for 5 min. Using a vacuum pump, the supernatant was removed, and this process was repeated three times to eliminate erythrocytes and achieve a whitish pellet. After processing, the pellet was resuspended in 100 µL of FACS buffer (DPBS, calcium, magnesium, ThermoScientific, 14040141 + BSA 0.1%) for subsequent incubation with antibodies. The infarcted area was dissected and digested with an enzyme cocktail (containing 50 U/ml collagenase, 8.5 U/ml dispase, 100 µg/ml Nα-tosyl-L-lysine chloromethyl ketone hydrochloride, and 5 U/ml DNase I in 9.64 mL HBSS1X (Gibco™ HBSS, no calcium, no magnesium, no phenol red, Fisher Scientific, 14175-095) for 30 min at 37°C. After digestion, the tissue was ground in a 2mL glass-glass grinder, filtered through a 70-µm filter, centrifuged, and the supernatant was discarded. The pellet was resuspended in 7mL of 35% Percoll, with 5mL of HBSS1X carefully layered on top to create a density gradient, and centrifuged at 4°C, 800g, for 30min without braking. After centrifugation, the myelin at the gradient interface, along with the rest of the supernatant, was discarded, leaving a pellet that was resuspended in 100µL of FACS buffer for staining. All the resulting suspension of cells was centrifuged at 650 x g, 4°C, for 5 min, the supernatant was discarded, and the pellet was resuspended in 100µL of FACS buffer.

Flow cytometry. Cell suspensions were stained with the following fluorochrome-conjugated monoclonal antibodies for 15 min at a concentration of 1:1000: anti-mouse Ly6G-PE (clone 1A8, BD Bioscience); anti-mouse CD45-FITC (clone 30-F11, BD Bioscience); anti-mouse/human CD11b-Brilliant Violet 510™ (clone M1/70, BioLegend); anti-mouse CD182 (CXCR2)-PerCP/Cy5.5 (clone SA044G4, BioLegend); anti-mouse CD184 (CXCR4)-APC (clone L276F12, BioLegend); anti-rat CD62L-FITC (clone MEL-14, BioLegend); anti-mouse Ly6C-FITC (clone HK1.4, BioLegend). After this incubation, 500 µL of DAPI at a concentration of 1:5000 in FACS buffer was added, and the samples were centrifuged at 650 x g, 4°C, for 5min, with the supernatant decanted. Finally, 400 µL of counting beads (BD Trucount™, Absolute Counting Tubes, BD, 663028) resuspended in FACS buffer at a concentration of 20 beads/µL and 100µL of FACS buffer were added, together with 100µL of FACS buffer, resulting in a final volume of 500 µL for analysis by flow cytometry. The staining strategy for analyzing neutrophils in the ischemic hemisphere was $CD45^{hi}$ $CD11b^{+}$ $Ly6G^{+}$. To analyze neutrophils in the blood the strategy used was $CD11b^{+}$ $Ly6G^{+}$. Doublets and $DAPI^{+}$ cells were excluded from analyses. Data were acquired using a FACS Canto or FACS LSRII Fortessa (BD Biosciences) and analyzed using FlowJo LLC software. Compensation was performed using single-labeled samples as reference and positive regions of staining were defined based on unstained and/or isotype-stained controls.

Neutrophil isolation by cell sorting. Blood was extracted and lysed as described in the organ processing section for flow cytometry. Cell sorting experiments were performed using a FACS Aria cell sorter (BD Biosciences). Neutrophils were isolated by selecting TdTomato-positive cells (from $Ly6G^{tdTom}$) in Catchup mice and as $DAPI^{-}$ $CD11B^{+}$ $Ly6G^{+}$ in C57BL/6 mice. Sorted neutrophils were collected in sterile Eppendorf tubes with 300 µL sorting buffer (Hepes 1M 1%, EDTA 0.5M 0.1%, FBS 1% in PBS 1X).

***Ex vivo* NET-formation assay.** Neutrophils were sorted as previously described; then, they were centrifuged at 650 x g for 4 min at 4°C. The supernatant was discarded, and cells were resuspended in and $5x10^4$ neutrophils were plated with RPMI medium (Gibco™ RPMI 1640, HEPES) on poly-l-lysine-covered 8-well µ-Slides (Ibidi) and left 30min to adhere. Subsequently, cells were incubated

for 2h with 100nM PMA or vehicle. Cells were then fixed using 4% PFA for 10min, permeabilized with PBS with 0.1% Triton X-100, 1% goat serum plus 5% BSA and stained with antibodies against cit-H3, DNA (Sytox-green, Molecular Probes) and MPO. Imaging of NETs was performed using a Zeiss LSM700 confocal microscope with 40x magnification, taking 5x5 tile-scan images with whole-slide Z-stack. We analyzed the images using Imaris (Bitplane) and identified NETs by the triple colocalization of the DNA, MPO and citH3 channels.

Quantification of primary granules. Neutrophils sorted as previously described and plated ($5x10^4$) with RPMI medium (Gibco™ RPMI 1640, HEPES) on poly-l-lysine-covered 8-well µ-Slides (Ibidi) were fixed using 4% PFA for 10 min. Afterwards, cells were stained with a biotinylated anti-MPO antibody (R&D Systems, 1:200) in PBS for 3 h at RT. Samples were then washed and incubated with Alexa-488 conjugated streptavidin in PBS for 1.5h at RT. Finally, cells were counterstained with DAPI (LifeTechnologies) to reveal nuclei. Granule images were collected using a Leica SP8 3X STED super resolution microscopy system coupled to a DMI6000 inverted microscope, with 100x magnification objective. Analysis of captured images was performed using Imaris (Bitplane) using the spots model in MPO channel.

Adoptive transfer experiments. Donor animals, $Bmal^{fl/fl}MRP8^{Cre+}$ and $Bmal^{fl/fl}MRP8^{Cre-}$ were injected intraperitoneally with 5 mg/kg of AMD-3100 (Sigma-Aldrich) 2 h before bleeding as described[6,11]. A control group of mice received similar volume of saline alone at the same time points. Following intracardiac bleeding of the donors, 20µL of blood was withdrawn to assess the effectiveness of the AMD treatment and estimate the number of neutrophils injected into the recipients. The extracted blood was then distributed by 150µL intravenously administration among different naive $Ly6G^{tdTom}$ recipient animals, 30min before starting MCAO surgery. After the surgeries, recipient animals received a second dose of 100µL of blood from their corresponding donor 5 h post-surgery.

Neutrophil elastase activity assay. Neutrophil elastase activity in plasma was measured using a commercially available kit (Neutrophil Elastase Activity Assay kit, Fluorometric, NAK246-1KT, Sigma-Aldrich) according to the manufacturer's instructions. We analyzed 50µl of plasma, with an excitation

wavelength of 390nm and emission wavelength of 510nm in a Fluoroskan Ascent plate reader (Thermo Labsystems). Standard curve goodness-of-fit had an R2 of 0.99 in linear regression.

Histology and tissue preparation. Mice were anesthetized and perfused intracardially with phosphate buffer (pH 7.4). The brain was removed, post-fixed with PFA overnight and cryoprotected in 30% sucrose. Finally, the brains were frozen using isopentane to proceed with sectioning on a microtome (Leica SM2000R). The sections were cut at a thickness of 30µm and stored in a cryoprotective solution, resulting in a total of 10 rostro-caudal series of sections per animal.

Immunofluorescence in tissue. Coronal brain sections from each mouse were placed in a 12-well plate where they were washed with 1X PBS for 5 min and incubated in blocking solution containing 5% bovine serum albumin (BSA) blocking solution in 1X PBS with 0.25% Triton-X for 1 hour at room temperature (RT) in agitation. After removing the blocking solution, immunofluorescence was performed on free-floating brain sections that were incubated overnight at 4°C with the following primary antibodies: anti mouse histone-3 citrulline (1:400, Abcam), anti-mouse/human myeloperoxidase (MPO) (1:200, R&D Systems), anti-mouse pan laminin biotinylated (1/250, Novus Biologicals), anti-mouse Ym1 (1/100, StemCell) and anti-mouse CD41 (1/200, Bioscience). The next day, after removing the primary antibody, the tissue was washed three times with 1X PBS + 0.25% Triton-X for 10 min per wash. Subsequently, the sections were incubated either with the corresponding streptavidin, in blocking solution at RT for 1h, or with the corresponding secondary antibody under the same conditions. The secondary antibodies used were anti-rabbit Alexa Fluor 647 (1:500, Thermo Fisher Scientific), anti-rat Alexa Fluor 647 (1:500, Invitrogen), streptavidin Alexa Fluor 488 (1:500, Thermo Fisher Scientific), streptavidin Alexa Fluor 405 (1:500, Thermo Fisher Scientific) and lectin 488-conjugated (1/100, Vector laboratories). Controls performed in parallel without primary antibodies showed very low levels of nonspecific staining. To rule out nonspecific secondary binding, negative controls were included in which the primary antibody was omitted and only the secondary antibody was applied. In addition, tissue known to lack the antigen was used as a negative control, while antigen-positive tissue served as a positive control. In some conditions, sections were incubated with DAPI (1:500, Life Technologies) at a 1:500 dilution in 1X PBS, followed by three washes with 1X

PBS to remove any residual DAPI. Sections were then mounted on gelatin-coated slides using Aqua-Plus Mount medium (18606-100, Polysciences) and allowed to dry overnight at 4°C in the dark.

Immunofluorescence in idibi plates. For immunofluorescence, the ibidi plates were washed three times for 10 min with 200 µL of 1X PBS. Blocking was performed with a blocking solution (1% NGS, 5% BSA, 5% FBS in 1X PBS with 0.1% Triton) for 30 min at RT. After the blocking solution was removed, the plates were washed three times with 200 µL of 1X PBS. Subsequently, the samples were incubated with primary antibodies: Anti-Myeloperoxidase (Goat, 1:200, 0400-0002, Bio-Rad) and Anti-Histone H3 (citrullinated R2 + R8 + R17) (Rabbit, 1:200, ab5103, Abcam) in a blocking solution and 1X PBS without Triton in equal proportions for 3 hours at RT. After removing the primary antibodies, the plates were washed three times with 1X PBS for 10 min with agitation. Then, 150 µL of secondary antibodies were added: Anti-Goat IgG (H+L) (Donkey, 1:500, A16003, Invitrogen) and Alexa Fluor 647 Anti-Rabbit (Chicken, 1:500, A-21443, Thermo Fisher), both in blocking solution and 1X PBS without Triton in equal proportions for 1 hour at RT. Later, the plates were washed three times for 10 min with 200 µL of 1X PBS. Next, a 1-hour incubation at RT was performed with Alexa Fluor 405 Streptavidin (1:500, catalog no. S32351, Invitrogen) prepared in 1X PBS. After removing the streptavidin, the plates were washed three times for 10 min with 1X PBS. In the final step, Sytox Green in 5 mM solution in DMSO (1:1000, S7020, Invitrogen) was added in 1X PBS for 10 min at RT, and each well was washed three times with 200 µL of 1X PBS. Both washing and incubation steps were carried out in conditions of darkness and humidity.

Image acquisition, processing and quantification in tissue. Acquisitions were performed with a laser-scanning confocal imaging system (Zeiss LSM700 in CNIC). Image quantification and analysis was performed with ImageJ and Imaris.

For NETosis analysis a 25x objective with immersion oil was used. MPO^+, $H3C^+$, and neutrophil $TdTomato^+$ were counted in confocal Z-stack images for which 3-5 serial sections (30µm) per animal spaced 300 µm apart were analyzed. Co-localization of these markers was considered positive for NETosis[17,23].

For ex vivo NETosis images, a 10x objective was used. DNA, H3C, and MPO were counted separately. Areas where the three markers co-localized or where they did not co-localize but neutrophil DNA expanded, adopting a cloud-like morphology, were considered positive for NETosis.

Cerebral blood flow assessment. Blood perfusion was evaluated by laser speckle contrast imaging (LSCI) (RFLSI-ZW, RWD). Animals were anesthetized as described in the ischemia models section and positioned in such a way that blood flow could be recorded in two regions: the lateral area of the skull where the MCA is located, and the superior area of the skull to record cerebral blood flow through the skull, after the overlying skin had been removed. These measurements were taken before performing the craniotomy and then for 5 min, after the craniotomy. Additionally, the superior area of the calvaria was recorded for 30 min following artery occlusion, while the MCA area was recorded for 5 min. Finally, the last blood flow measurements were taken 12 h after the occlusion, with 5-minute recordings in both aforementioned areas. Blood flow was measured with the software RFLSI Analysis.02.00.31.29469.

Neutrophil depletion. To deplete neutrophils at ZT5, 2 groups of mice were injected with either mouse anti-neutrophil antibody (anti-mouse Ly-6G 1A8 clone, which is specific to neutrophils within myeloid cells, BE0075, BioXCel; 0,4mg per day i.p.) or control isotype (rat IgG2A, BE0089, BioXCell) daily for 4 days, starting 24 h before surgery. The anti-Ly6G antibody used has been previously demonstrated to induce neutropenia with minimal changes in other blood cell populations[22].

***In vivo* treatments.** *Chloramidine administration:* Chloramidine (Cayman Chemical Company, VITRO) was dissolved in DMSO and saline and a dosage of 50mg/kg was intravenously administered 10 min before and after MCAO. A second group of mice received similar volume of PBS alone at the same time points as control group. *DNase-I treatment:* DNase-I (recombinant human DNase-I protein) 10µg was administered intravenously, followed by an intraperitoneal injection of 50µg/250µL of the same compound 3 and 12 h after occlusion[17].

Assessment of neurological deficits by the footprint test. The gait pattern in mice was assessed through footprint test as described[98]. Briefly, the fore and hind feet of the mice were painted with blue

and green nontoxic paints, respectively. Animals were then allowed to freely walk along a narrow corridor (50x10x10 cm). Fresh sheet of white paper was placed on the floor of the runway for each run. The footprint patterns were analyzed for four step parameters (all measured in cm). Forelimb stride length was measured as the average distance of forward movement between each stride.

Single cell RNA sequencing (scRNA-sequencing) of sorted tissue neutrophils. Brain neutrophils ($CD11b^+$ $Ly6G^+$ $DAPI^-$) were isolated using a FACS Aria Fusion sorter (BD Bioscience), as detailed in the gating strategy flow-chart (Suppl. Fig. 6), collected into 0.04% BSA/PBS and loaded into a BD Rhapsody cartridge. Pools of cells ten mice were created for each brain group. Up to 60.000 cells were loaded into a Rhapsody Single Cell Analysis System cartridge. Cell captures and cDNA synthesis were performed according to manufacturer's instructions. The pool of all samples of labelled Sample Tags cells was checked for viability and cell concentration using the Countess III cell counter (Thermofisher). The average size of the libraries was calculated using the 2100 Bioanalyzer (Agilent) and the concentration was determined using the Qubit® fluorometer (Thermofisher). Finally, libraries were combined and sequenced together in a paired end run (60x42) using a NextSeq 2000 system (Illumina) and a P2 flowcell. Output files were processed with NextSeq 1000/2000 Control Software Suite v1.4.1. FastQ files for each sample were obtained using BCL Convert v3.6.3 software (Illumina). NGS experiments were performed in the Genomics Unit of the CNIC.

Sequence alignment, unique molecular identified (UMI) quantification, and single-cell identification were performed using the Rhapsody Whole Transcriptome Analysis pipeline (version 1.12.1), based on the mouse GRCm39 genome assembly and Ensembl genebuild (version 108). Single cells were filtered and clustered using scuttle (v1.10.3)[99] and Seurat (v4.40)[100] R packages. Cells were filtered using a sequencing depth between 1500 and 20,000, a minimum of 800 detected genes, a mitochondrial content below 10%, a gene expression complexity (percentage of reads from the top 50 genes) below 50%, a hemoglobin gene set expression below 1% and a HTO content above 50 UMIs in the hashtags. Doublets were identified using scDblFinder (v1.14.0)[101] and were removed. Mitochondrial and hemoglobin genes were excluded for downstream analysis. At the end of the filtering process, a total of 6522 cells were retained.

Counts were normalized, and the most variable 1000 genes were identified using VST. All samples were integrated using Seurat's IntegrateData function with RPCA method. Clustering and dimensionality reduction of these cells were performed using *15* principal components. Cluster markers and differential expression analysis between conditions have been performed using Wilcox algorithm, testing only genes detected in more than 30% of cells for markers and 10% for differential expression on any cluster. Functional analysis was performed using enrichR (v.3.2)[102] to identify enriched pathways between conditions.

Blinding procedures. Analyses and quantification of histology, immunofluorescence, MRI, LSCI, behavioral outcomes, and flow cytometry were performed on coded samples or datasets by investigators blinded to group allocation. Similarly, biochemical assays were processed with coded samples. Surgical procedures could not be blinded due to timing requirements, but all subsequent data analyses were performed by independent, blinded evaluators.

Statistical analysis of preclinical data. Statistical analyses were performed using Prism 10 (GraphPad Software Inc.) and the R statistical computing environment (version 4.3.0; R Foundation for Statistical Computing, Vienna, Austria) and additional specialized packages (ggplot2, dplyr, tableone, broom, ggpubr, and cosinor (version 1.2.3). Prior to applying any statistical test, data were assessed for normality using Shapiro–Wilk test. If the data met the assumption of normality, parametric tests were applied. In cases where data did not follow a normal distribution, or when the sample size was $n<6$, non-parametric alternatives were employed. For comparisons between two groups, normally distributed data were analyzed with an unpaired t-test, while non-normally distributed data were compared using the Mann–Whitney U test. For comparisons among more than two groups with a single independent variable, one-way ANOVA was used if assumptions were met; otherwise, the Kruskal–Wallis test was applied, followed by Dunn's post hoc test for pairwise comparisons. For analyses involving two independent variables, a two-way ANOVA was performed when data met normality assumptions. When data violated these assumptions, we employed ART ANOVA (Aligned Rank Transform ANOVA) and the Scheirer–Ray–Hare test, to examine main effects and interactions in our factorial design, providing a robust non-parametric alternative when normality

assumptions are not satisfied. For post hoc comparisons between groups, we applied Emmeans, Kruskal–Wallis tests with Dunn's correction and, Mann–Whitney U tests with Holm–Šídák correction. All statistical analyses included corrections for multiple comparisons using statistical hypothesis testing. Diurnal oscillations of infarct size in Fig.1 were assessed using Cosinor analysis, which provided estimates for MESOR, amplitude, acrophase, and p-values to determine significant diurnal patterns ($p<0.05$). All statistical data were represented as the mean ± SEM, and in all studies, tests were considered significant when $p<0.05$. Excluded values from the study were identified and removed using various outlier detection criteria. The Grubbs' test ($\alpha=0.05$) was applied to exclude extreme values when only one value was considered an outlier. Additionally, the ROUT method ($Q=1\%$) was used, and in certain cases, exclusion was based on the interquartile range (IQR), excluding values lower or higher than 1.5 times the IQR when the sample size was between 3 and 5.

Clinical study design and patient cohort. This study included a total of 540 patients admitted to the stroke unit of Hospital 12 de Octubre (Madrid, Spain) between January 2018 and July 2024. All patients met the general inclusion and exclusion criteria detailed below.

Inclusion Criteria: Patients aged over 18 years with an ischemic stroke, previously independent (pre-morbid modified Rankin Scale -mRS- < 2), and admitted within six hours of symptom onset or after a wake-up stroke.

Exclusion Criteria: Patients with transient ischemic attacks (TIA), lacunar strokes, intracranial bleeding secondary to trauma or subarachnoid hemorrhage, or with a history of stroke, acute myocardial infarction, severe systemic infection, or major surgery within the last three months were excluded. Additional exclusion criteria included active severe systemic inflammatory disease, pregnancy, or puerperium.

Circadian rhythm subcohort: For the circadian rhythm analysis, a subset of 366 patients was selected from the main cohort based on the additional inclusion criterion of a witnessed stroke with a known symptom onset time. This subcohort, therefore, comprised patients with an ischemic stroke of known

onset. Data on both the time of symptom onset and time of hospital admission were recorded for each patient to allow precise circadian analysis.

Collateral circulation subcohort: A subcohort of 310 patients from the main cohort was used to study collateral circulation. This subcohort included patients with both wake-up strokes and those with unknown symptom onset times to maximize sample size. Collateral circulation was assessed by neurologists using cerebral angiography imaging, such as computed tomography angiography (CTA) or magnetic resonance angiography (MRA). The ASITN/SIR scale (American Society of Interventional and Therapeutic Neuroradiology/Society of Interventional Radiology), which categorizes collateral circulation into five grades (0: no collaterals; 1–4: increasing degrees of collateral supply), was employed. For analysis, collateral circulation was categorized as "poor" (grades 0–2) or "good" (grades 3–4).

Control cohort consisted of 37 individuals without acute neurological conditions, matched to the stroke cohort for age, sex, and vascular comorbidities ("old controls"). Additionally, a second control group comprised young individuals without vascular comorbidities ("young controls").

Data collection and laboratory variables: Data on age, gender, cardiovascular risk factors (CVRF), prior medication were collected for all patients and controls. Baseline stroke severity (National Institutes of Health Stroke Scale, NIHSS) was assessed in patients. Laboratory data, including biochemistry, cell counts (lymphocytes, leukocytes, neutrophils, platelets, mean platelet volume) and coagulation parameters were obtained from the blood samples. Additionally, data regarding patient management, NIHSS scores at the stroke unit, infarct volumes, and 90-day mRS outcomes were retrospectively retrieved from hospital discharge and follow-up records. Neurologists measured the infarct volume for each patient using computed tomography (CT) and magnetic resonance imaging (MRI) scans obtained within the first 48 hours post-stroke. The infarct volumes were assessed in a double-blind manner to ensure objectivity and reduce assessment bias.

Blood sample collection and biomarker quantification: Whole blood treated with EDTA was collected upon admission and again 12–24 hours after admission while in the stroke unit. Plasma was extracted

from these samples for quantification of neutrophil-specific elastase (NE), myeloperoxidase (MPO), and soluble CD40 ligand (sCD40L). Quantification was performed using commercially available enzyme-linked immunosorbent assay (ELISA) kits following the manufacturers' instructions: Human PMN Elastase ELISA kit (Abcam, Cambridge, MA, USA), Human MPO ELISA kit (R&D Systems, Minneapolis, MN, USA), and Human CD40L (Soluble) ELISA Kit, Extra Sensitive (Thermo Fisher Scientific, Waltham, MA, USA).

Statistical analysis of clinical data: All analyses were conducted using the R statistical computing environment (version 4.3.0; R Foundation for Statistical Computing, Vienna, Austria) and additional specialized packages (ggplot2, dplyr, tableone, broom, ggpubr, and cosinor (version 1.2.3)). Missing values were analyzed as 'missing' without imputation due to the substantial proportion of missing data in certain post-stroke variables, which violated the assumptions required for robust and unbiased imputation methods. For variables with non-normal distributions, such as neutrophil elastase and myeloperoxidase (MPO), logarithmic transformations were applied to normalize the data. Normality was reassessed post-transformation using visual (QQ-plots) and statistical methods. Circadian rhythm analysis was performed using the cosinor package to model diurnal variations in biomarkers, NIHSS scores, infarct volumes, and hematological cell counts (lymphocytes, leukocytes, neutrophils, and platelets). The analysis provided estimates of MESOR (midline estimating statistic of rhythm), amplitude, and acrophase for each variable. Amplitude was of particular interest, as it reflects the extent of variation across the circadian cycle. A significant amplitude ($p<0.05$) indicates a meaningful fluctuation in levels over 24 hours, which may reveal underlying circadian regulation mechanisms relevant to ischemic stroke outcomes. In the collateral circulation study, comparisons were made between "poor" and "good" collateral groups. Parametric or non-parametric tests were used as appropriate for each variable after applying an interquartile range (IQR) filter to identify and exclude outliers; differential significance was set at a p-value<0.05. Sensitivity analyses confirmed that the exclusion of outliers did not alter the robustness of the results. Potential confounders were assessed using statistical tests, and no significant imbalances were detected between groups.

Sample size justification: This study is pioneering in evaluating diurnal patterns of immunothrombosis biomarkers, NIHSS scores, infarct volumes, and hematological cell counts in an Iberian cohort of patients with ischemic stroke. Due to the absence of prior studies in our target population using these specific markers and variables, a formal sample size calculation based on previous estimates was not feasible. However, we established a statistical significance level of $\alpha = 0.05$ and a statistical power of 80% to detect clinically relevant differences. To enhance the sample size and improve statistical power in the study of collateral circulation and circadian patterns, we included patients with wake-up strokes and those with unknown symptom onset times. This decision was made because the evaluation and collection of collateral circulation grades and certain clinical parameters were not performed in all patients of the study. Although the inclusion of these patients may introduce some variability, we performed sensitivity analyses to ensure that this variability did not bias the results. This approach was deemed necessary to achieve a sufficiently large and representative sample size for robust statistical analyses.

Ethical approval and informed consent: This study was approved by the Institutional Review Board (IRB) of Hospital 12 de Octubre. Informed consent (CEIM 60/204) was obtained from all patients or their legal representatives prior to inclusion in the study, in compliance with institutional and ethical guidelines for human research.

Online Figures S1-S16

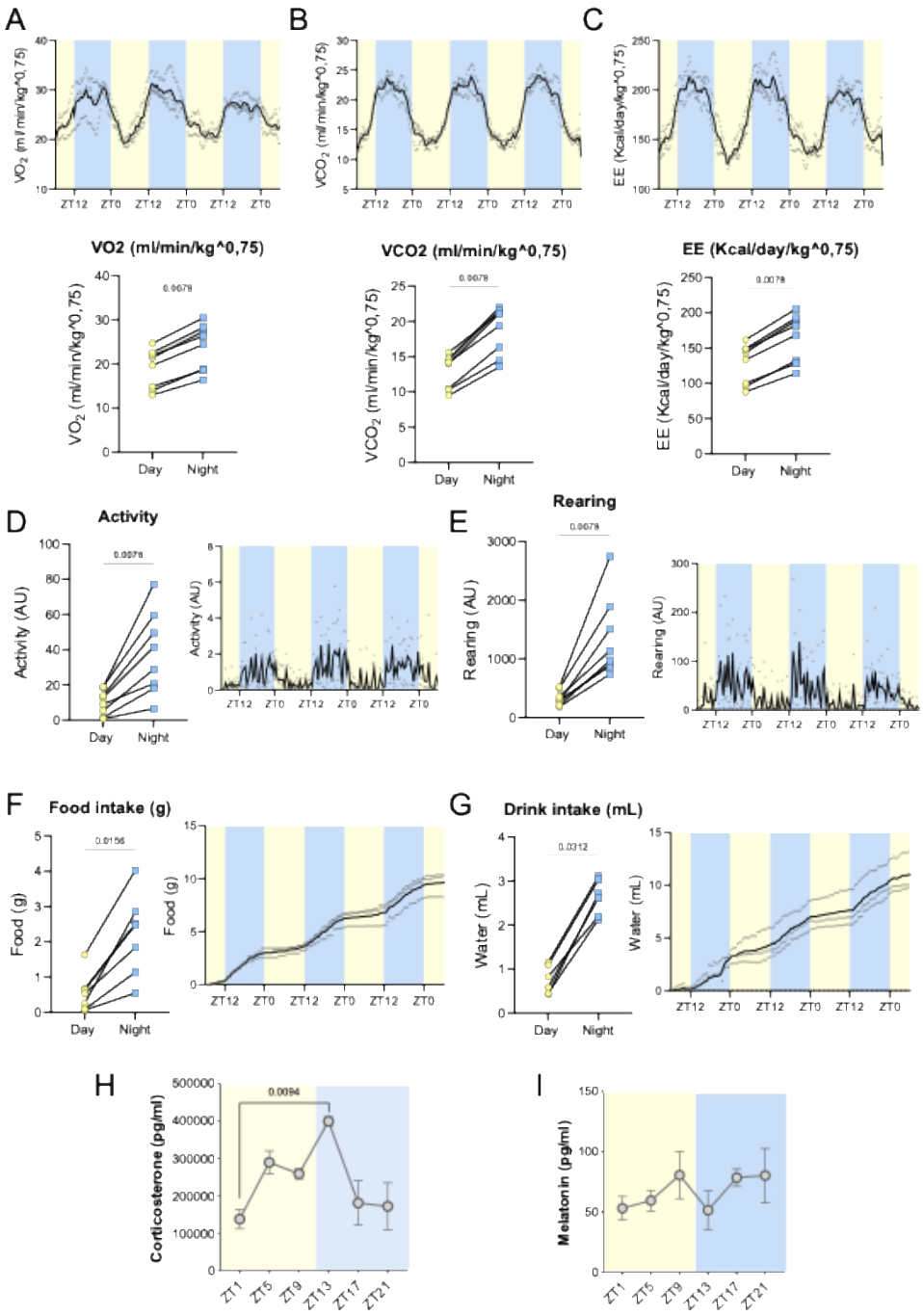

Supplementary Figure 1. Circadian rhythmicity of metabolic and behavioral parameters in wild-type mice. Oxygen consumption (VO_2), carbon dioxide production (VCO_2), energy expenditure (EE), general locomotor activity (activity), vertical activity (rearing), food intake, and water intake were continuously recorded in wild-type C57BL/6J mice housed individually in metabolic cages for 3 consecutive days with *ad libitum* access to food and water. Data are plotted as mean ± SEM. Light (yellow) and dark (blue) phases are indicated. AUs: Arbitrary Units. Panels A-E: Comparison between day and night (n=8 in a single experiment) using a non-parametric paired test (Wilcoxon); *p=0.0078. Panel F: Wilcoxon test, *p=0.0156. Panel G: Wilcoxon test, *p=0.0312. Panels H-I: Comparison across ZT1, ZT5, ZT9, ZT13, ZT17 and ZT21 (n=4, 5, 4, 5, 5, 3, respectively) using a Kruskal-Wallis test. Panel H: p=0.0086, Dunn's post hoc test showed a significant difference between ZT1 and ZT13 (*p=0.0094). Panel I: Kruskal-Wallis test, p=0.4251 (not significant). Data represent mean ± SEM.

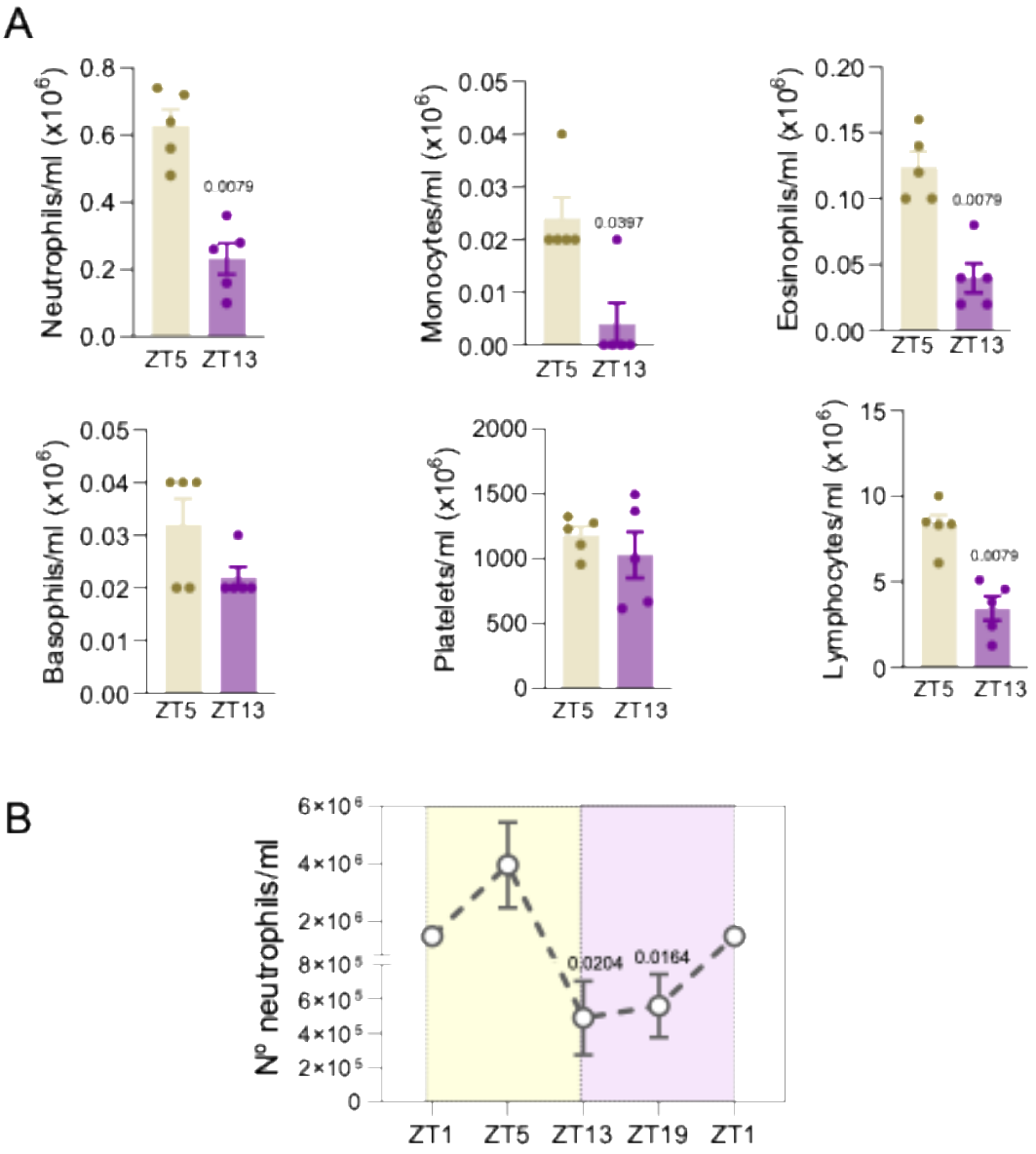

Supplementary Figure 2. Time-dependent variation in leukocyte populations in peripheral blood of mice. (A) Complete blood count (CBC) analysis revealed significant reductions in total leukocyte numbers at ZT13 compared to ZT5, with neutrophils showing the most pronounced decrease. Comparison between ZT5 (n=5 in a single experiment) and ZT13 (n=5 in a single experiment) was performed by non-parametric Mann Withey test. Neutrophils (*p=0.0079); Monocytes (*p=0.0397); Eosinophils (*p=0.0079); Lymphocytes (*p=0.0079). (B) Flow cytometry analysis of neutrophils at ZT1, ZT5, ZT9, ZT13 and ZT19 (n=6, 5, 5, 7 and 6 respectively in a single experiment per ZT), highlighting the circadian regulation of immune cell distribution. Data was compared by using a Kruskal-Wallis test (p=0.0015). Dunn's post hoc test showed a significant difference between ZT5 vs. ZT13 (*p=0.0204) and ZT5 vs. ZT19 (*p=0.0164). Data represent mean ± SEM.

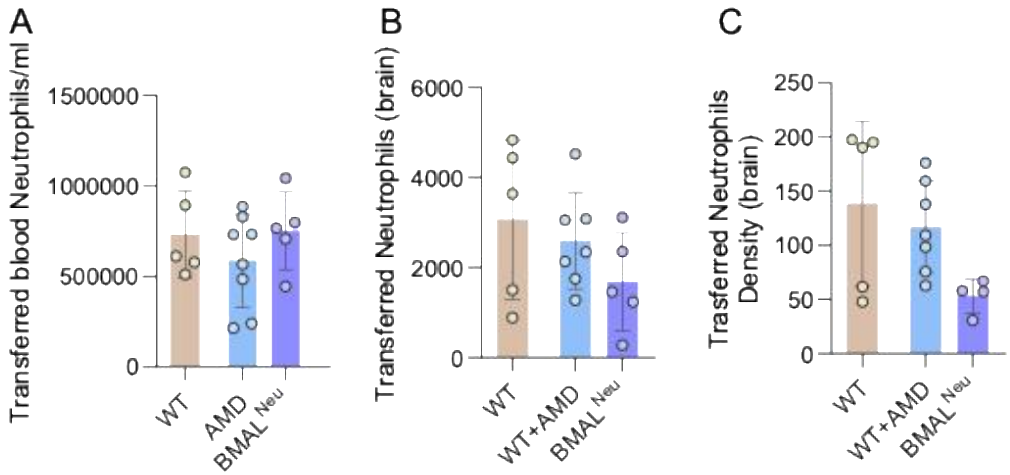

D

	30 min before stroke		4 h after stroke	
Donor	**Blood volume (µl)**	**Neutrophils (Mean)**	**Blood volume (µl)**	**Neutrophils (Mean)**
WT	120	68,992	100	82,814
WT + AMD	120	969,422	100	571,275
BMAL^{neu}	150	757,000	100	627,822

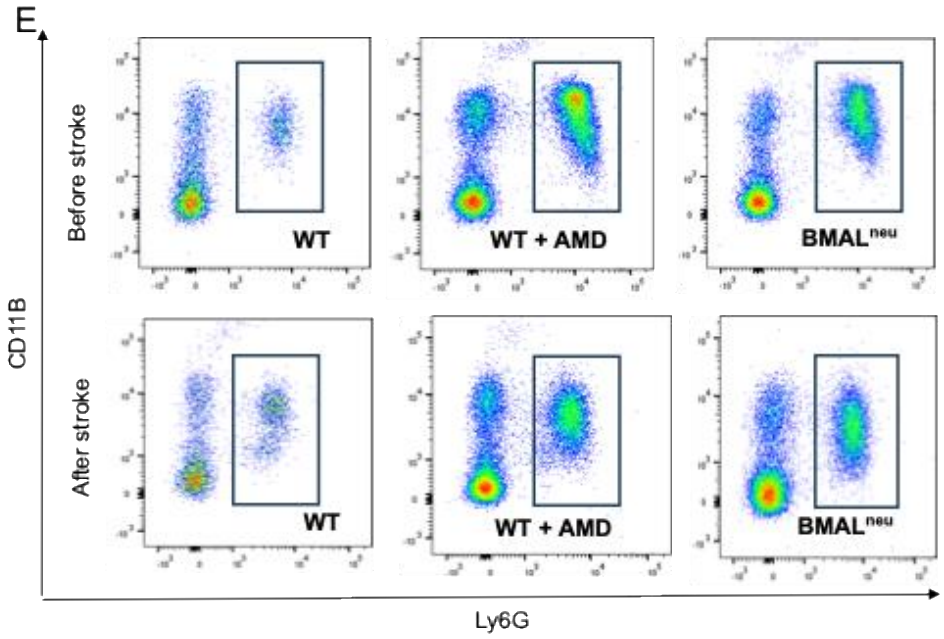

Supplementary Figure 3. Quantification and flow cytometry analysis of transferred neutrophils. (A) Quantification of transferred blood neutrophils/ml, (B) transferred brain neutrophils and (C) transferred neutrophils density from donors in receptor animals 24 hours after ischemia in WT group, AMD+WT group and Bmal^{neu} group. (D) Summary table with the number of neutrophils transferred from each group in the two injections performed for each mouse (before stroke and after stroke). (E) Representative cytometry dot plots of blood neutrophils from each of the donor groups (WT, WT + AMD and Bmal^{neu} group) in both the pre-ischemia and post-ischemia injections. Neutrophils were gated as DAPI^{-}CD11B^{+}Ly6G^{+}. Data in (A-C) was compared by using a Kruskal-Wallis test. No significant differences were observed. WT (n=5 in a single experiment), WT + AMD (n=7 in 2 independent experiments) and Bmal^{neu} (n=5 in a single experiment). Data represent mean ± SEM.

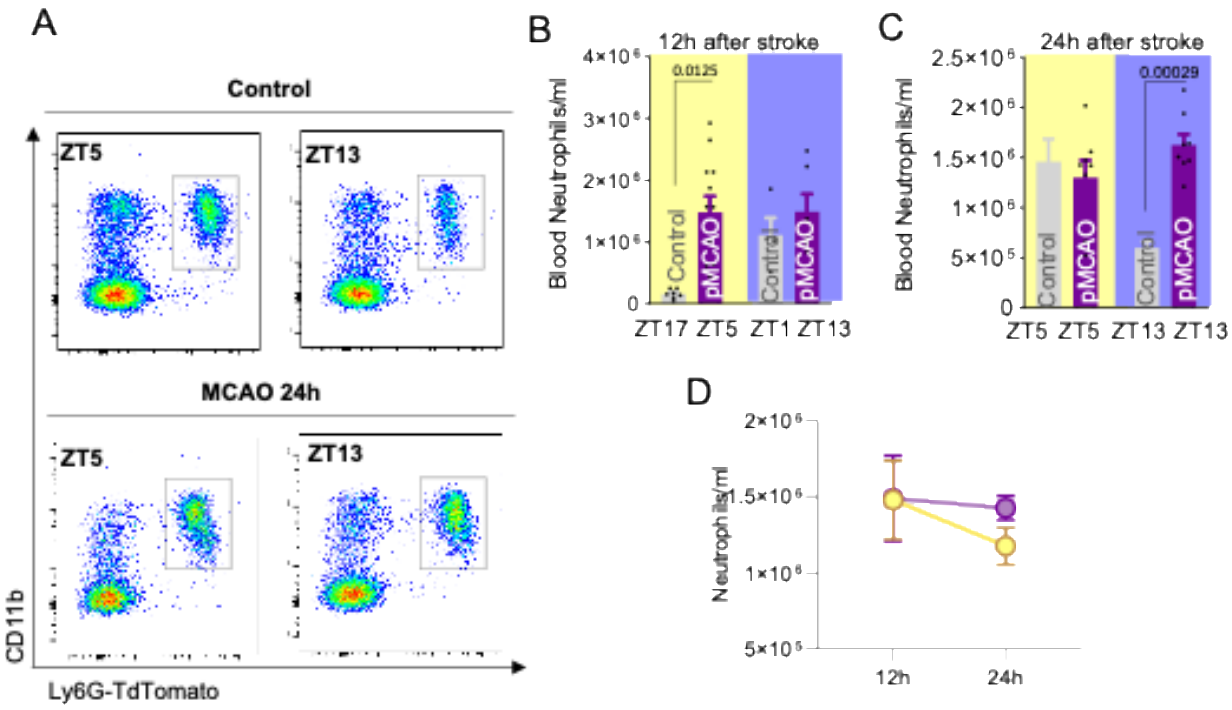

Supplementary Figure 4. Analysis of blood neutrophils at different times after stroke. (A) Representative flow cytometry plots of blood neutrophils from control and pMCAO mice 24 hours after stroke at both ZT5 and ZT13. Neutrophils are gated as DAPI-CD45+CD11B+Ly6G+. (B) Blood neutrophil quantification (neutrophils/ml) in naïve control group (at ZT17 (n=7) and ZT1 (n=4)) and 12 hours after MCAO group (subjected to surgery at ZT5 (n=12 in 2 independent experiments) and ZT13 (n=6 in a single experiment)). (C) Blood neutrophil quantification (neutrophils/ml) in naïve control group (at ZT5 (n=7 in a single experiment) and ZT13 (n=13 in 2 independent experiments)) and 24 hours after MCAO group (stroke at ZT5 (n=8 in a single experiment) and ZT13 (n=8 in a single experiment)). Data in B and C were compared by non-parametric ART ANOVA followed by Emmeans post hoc. At 12h (B), a significant effect was detected for surgery ($F(1,24)=11.738$, $p=0.0022$). Naive ZT17 vs. ZT5 MCAO (*$p=0.0416$). At 24h (C), a significant interaction between stroke and circadian time was observed ($F(1,32)=20.483$, $p=7.82\times10^{-5}$). Naive ZT13 vs. ZT13 MCAO (*$p=0.00029$). (D) Comparison of blood neutrophil numbers 12 and 24h after stroke in mice subjected to surgery at ZT5 (in yellow) and ZT13 (in purple). ZT1 and ZT17 were used as naïve controls to match the circadian phase of mice analyzed 12 h after surgery at ZT13 and ZT5, respectively. Data represent mean ± SEM.

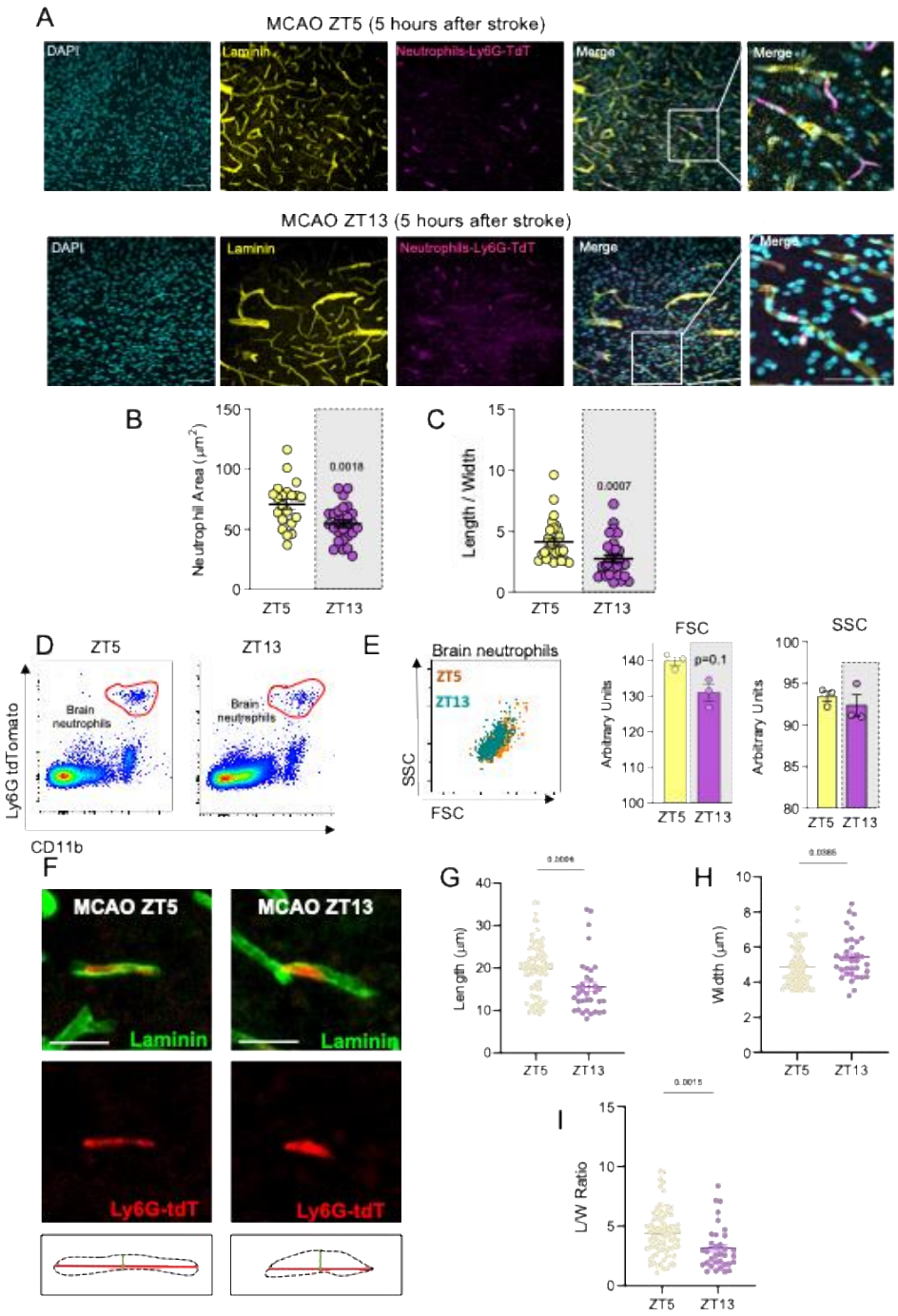

Supplementary Figure 5. Neutrophil morphology in the ischemic brain differs between ZT5 and ZT13 at 5 and 12h post-MCAO. (A) Representative immunofluorescence images of brain neutrophils 5 hours post-MCAO, taken from both ZT5 and ZT13 ischemic mice. Nuclei stained with DAPI and are shown in cyan, blood vessels labeled with laminin are shown in yellow, and neutrophils expressing TdTomato from Catchup mice are shown in magenta. Scale bar=25 µm. (B) Quantification of the size of brain neutrophils estimated as the area (µm^2) 5 hours post-MCAO, taken at both ZT5 (n=21 in a single experiment) and ZT13 (n=27 in a single experiment). Data were compared by an unpaired t test (*p=0.0018). (C) Estimation of the length / width ratio for each brain neutrophil from ZT5 (n=27) and ZT13 (n=30) ischemic mice 5h after stroke. A non-parametric Mann Whitney test was performed (*p=0.0007). (D) Representative flow cytometry plots of brain neutrophils from ZT5 and

ZT13 ischemic mice 5h after stroke. Neutrophils are gated as $DAPI^{-}CD45^{+}CD11B^{+}Ly6G^{+}$. (E) Representative flow cytometry plots displaying SSC and FSC parameters of brain neutrophils from ZT5 (n=3 in a single experiment) and ZT13 (n=3 in a single experiment) ischemic mice 5h after stroke. Right: quantification of the mean FSC and SSC parameters estimated as arbitrary units (AU) in brain neutrophils from ZT5 and ZT13 ischemic mice 5 hours post-MCAO. Data were analyzed by Mann Whitney test. (F-I) Quantification of neutrophil length, width, and length-to-width ratio (L/W) in the ischemic brain 12h after transient ischemia induced at ZT5 (n=67) or ZT13 (n=34). Neutrophils were identified by endogenous tdTomato expression in Catchup mice, which selectively label neutrophils. Neutrophils from mice subjected to ischemia at ZT13 displayed significantly reduced length along with a higher L/W ratio compared to those at ZT5, indicating a more rounded morphology. These data support time-of-day-dependent differences in neutrophil behavior and morphology within the injured brain. Data were analyzed by Mann Whitney test (G, *p=0.0006; H, *p=0.0385 and I, *p=0.0015). Scale Bar= 10µm. Data are shown as mean ± SEM.

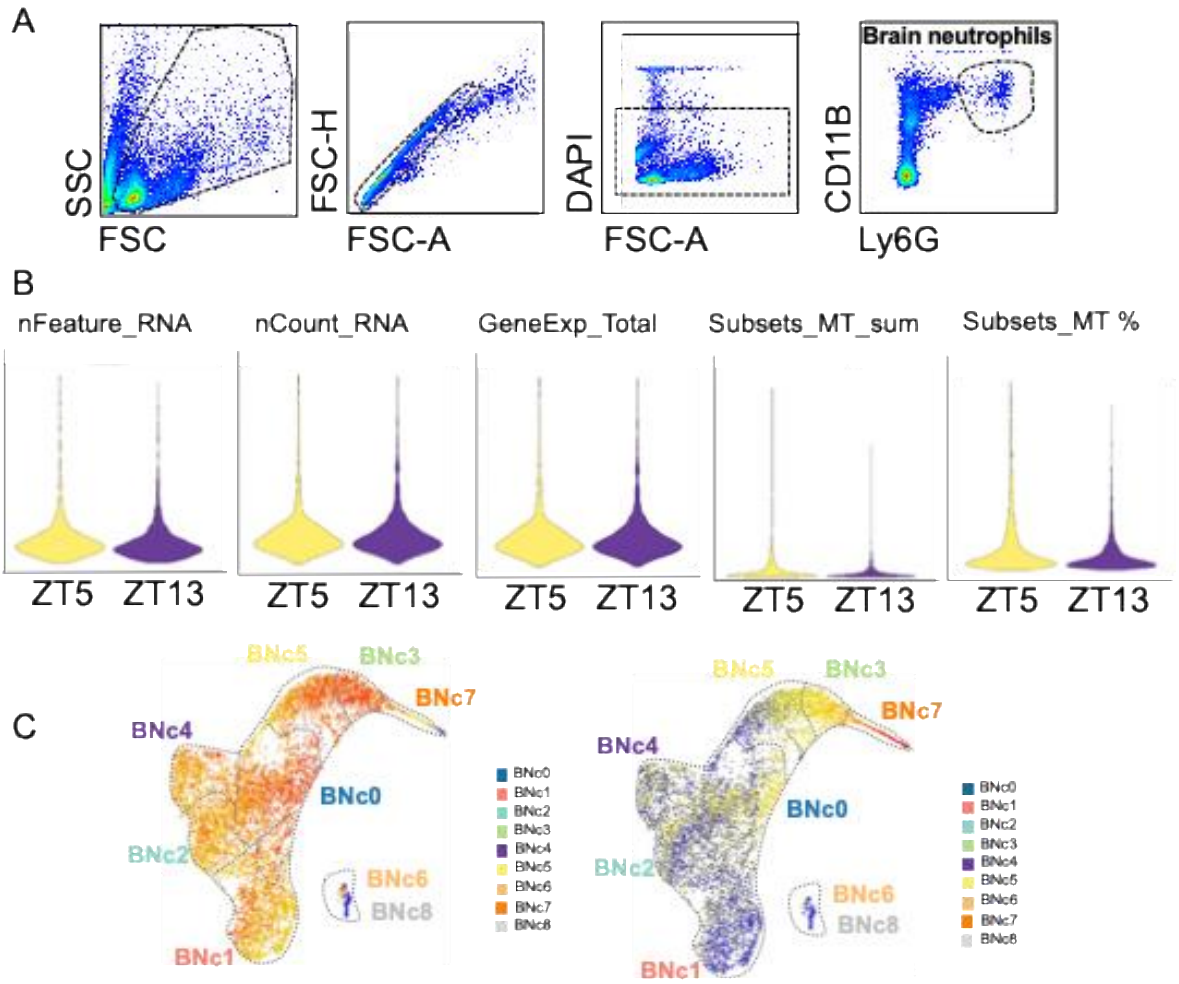

Supplementary Figure 6. Quality assessment of brain neutrophils for scRNA-seq analysis. (A) Gating strategy for sorting of brain neutrophils 12h after stroke in both ZT5 (n=9 in a single experiment) and ZT13 (n=9 in a single experiment) ischemic mice. Neutrophils were sorted as $CD45^{hi}$, $CDb11^{+}$, $Ly6G^{+}$, $DAPI^{-}$. (B) Violin plots of the number of genes, feature RNA, RNA counts, number of UMIs and percentage of mitochondrial UMIs. (C) UMAPs of the 3351 brain neutrophils colored by z-score scaled expression showing that BNc7 is the one with high bone marrow proximity score (right) and low maturation score (left).

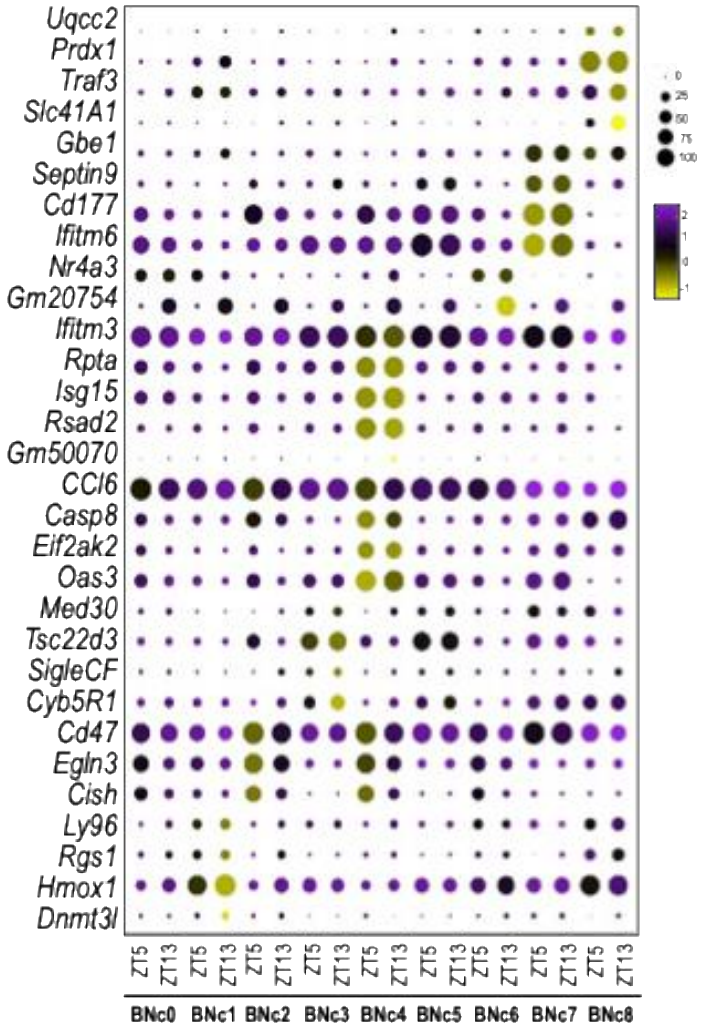

Supplementary Figure 7. Differentially expressed genes of brain neutrophil ZT5 and ZT13 subsets. Dot plot showing the scaled expression of signature genes for each cluster that significantly changes between ZT5 (n=9 in a single experiment) and ZT13 (n=9 in a single experiment) ischemic mice, colored by the average expression of each gene in each cluster scaled across all clusters. Dot size represents the percentage of cells in each cluster with more than one read of the corresponding gene.

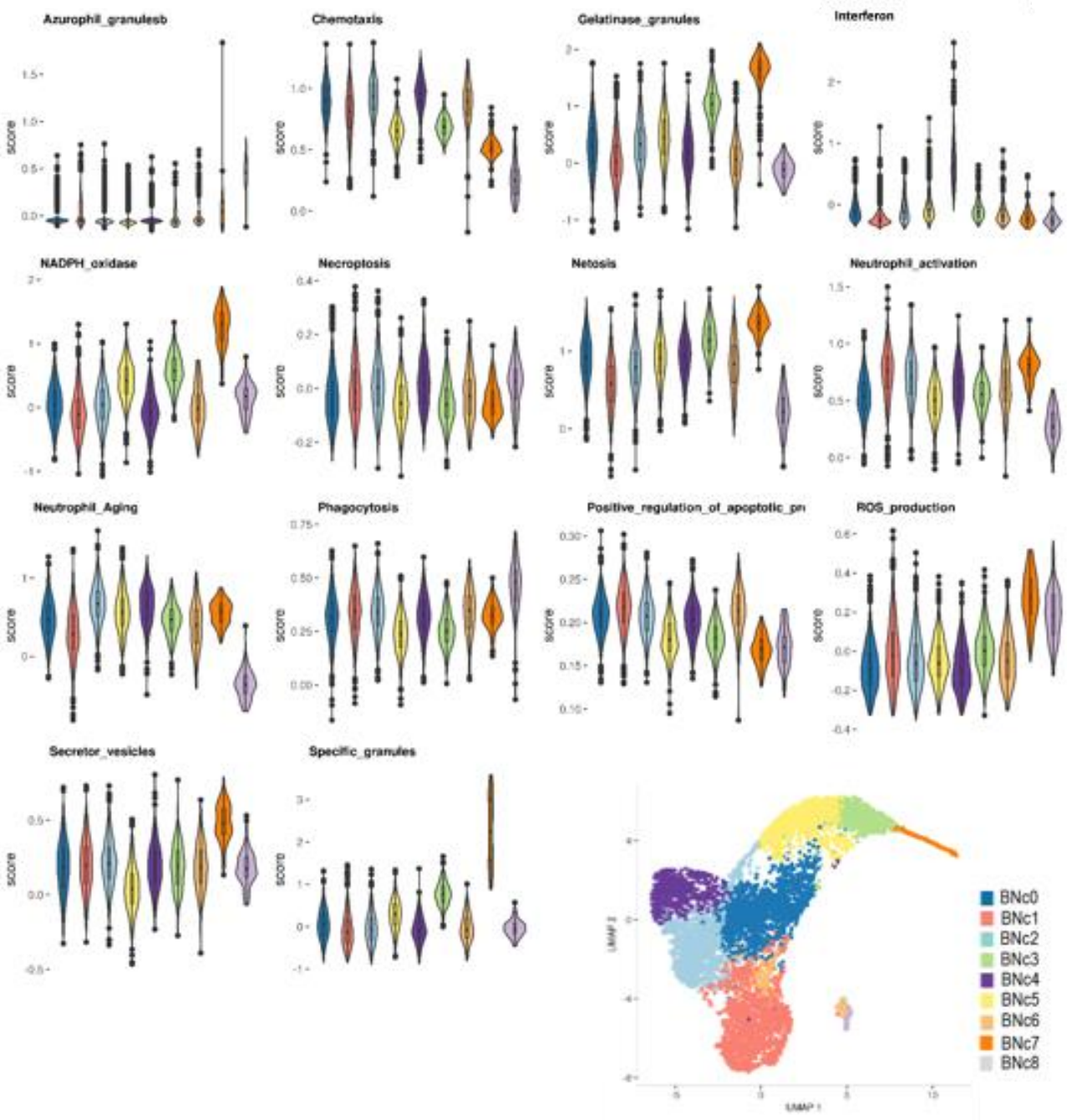

Supplementary Figure 8. Transcriptional profile of different brain neutrophil subsets for various core and effector neutrophil functions. Violin plots of different scores for neutrophil effector functions defined as weighted average Z-scores of effector function-related genes previously described in the literature (Extended Data Table S2) for different BNCs detected in the brain.

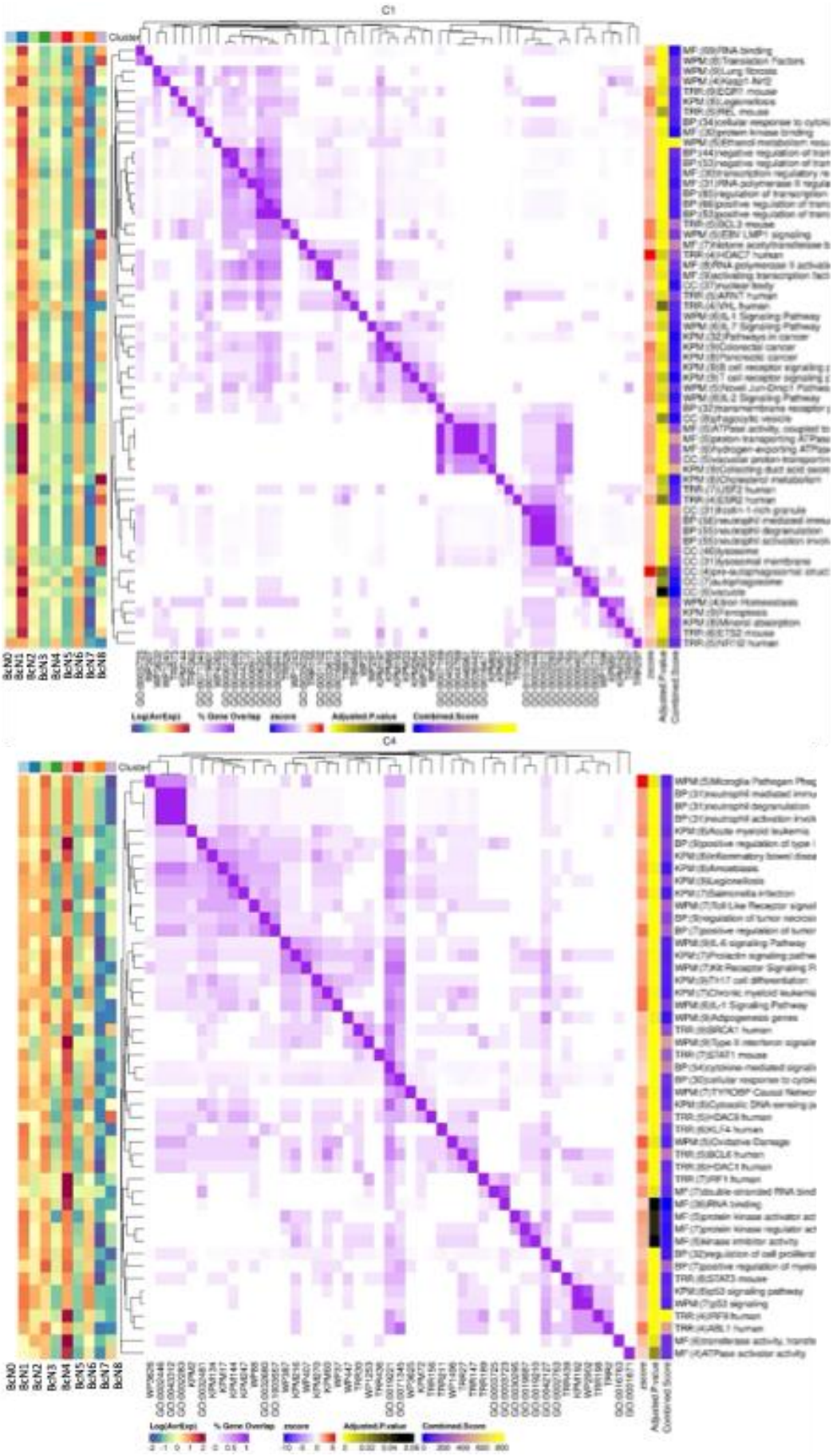
C1
Cluster
BcN0
BcN1
BcN2
BcN3
BcN4
BcN5
BcN6
BcN7
BcN8
Log(AvrExp)
% Gene Overlap
zscore
Adjusted P-value
Combined Score
C4

Supplementary Figure 9. Functional gene ontology analysis of DEGs in clusters BNC1 (top) AND BNC4 (bottom). Heatmaps hierarchical clustering of gene expression levels and gene ontology analysis showing the correlation matrix of GO analysis for each cluster. The dendrogram shows the Euclidian distance between samples, while the heatmap shows the Pearson correlation (purple = 1, white = −1).

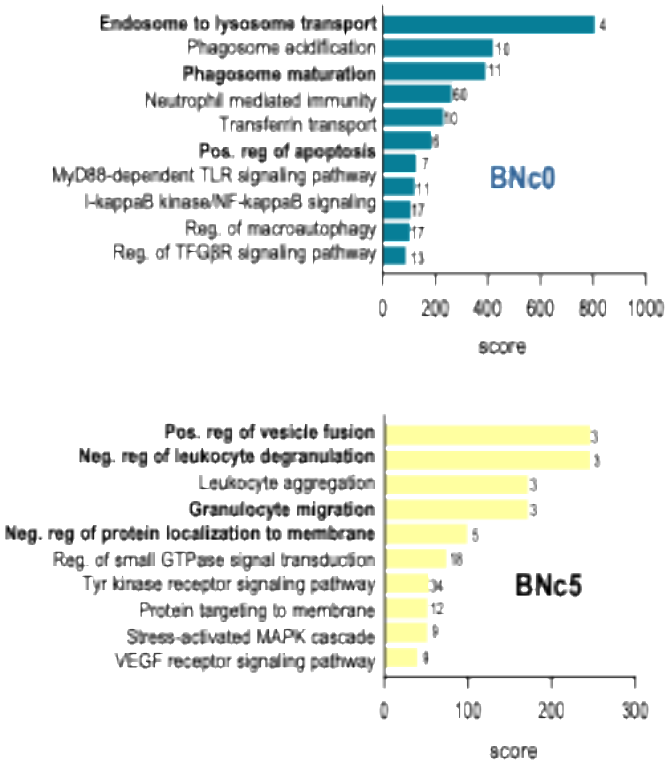

Supplementary Figure 10. Gene ontology analysis of DEGs for the clusters BNc0 (top) and BNc5 (bottom). The graph shows selected gene ontology terms with Benjamini–Hochberg-corrected p-values<0.05 and ordered by combined score.

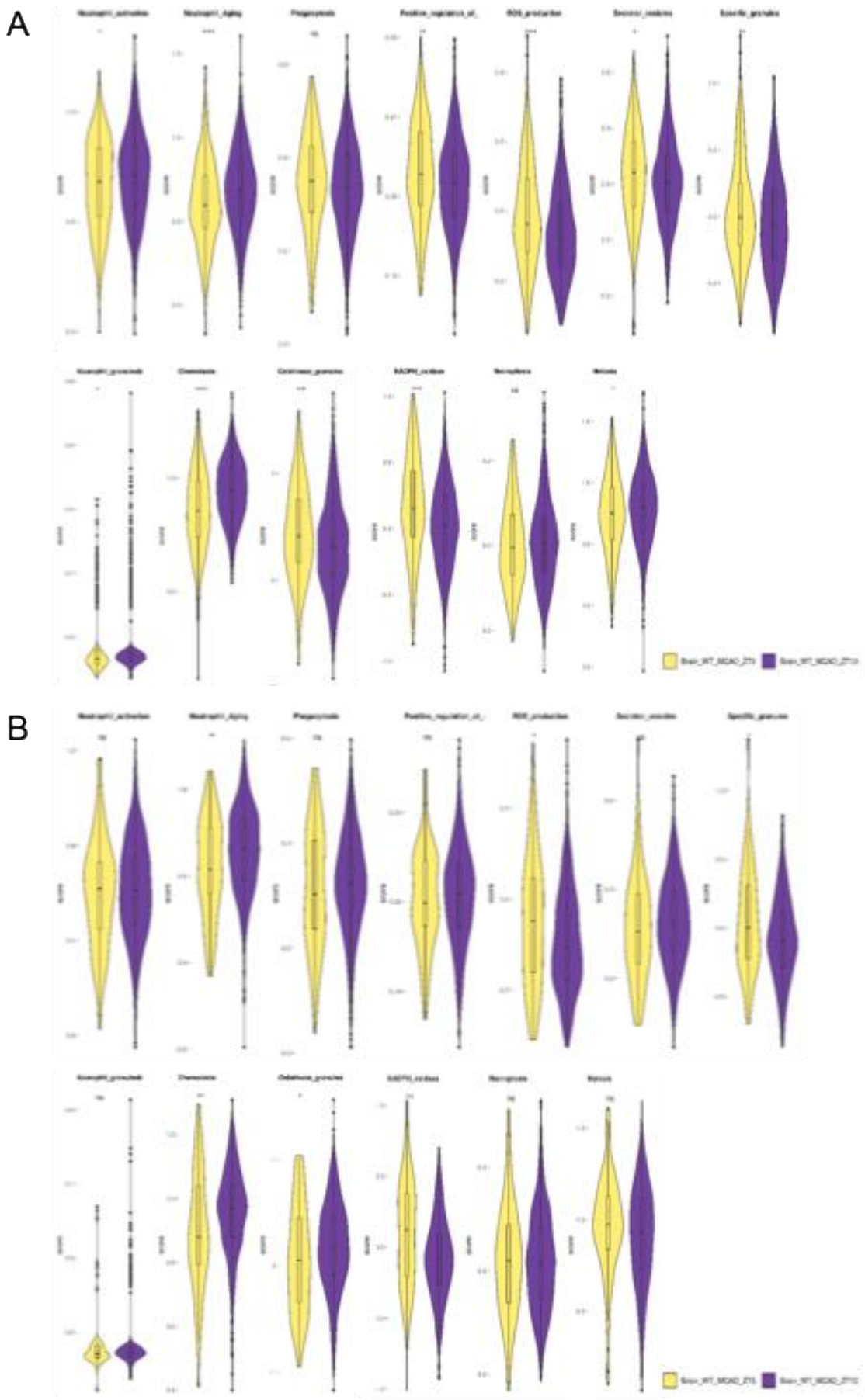
A
B

Supplementary Figure 11. Functional profiling of BNc2 and BNc4 brain neutrophils across circadian time points. Violin plots showing the distribution of functional scores for key neutrophil-related processes in cluster BNc2 (A) and BNc4 (B) at ZT5 (yellow) and ZT13 (purple). Scores reflect gene set activity for each annotated function, including granule types, chemotaxis, oxidative burst (NADPH oxidase), neutrophil activation, aging, NETosis, and others.

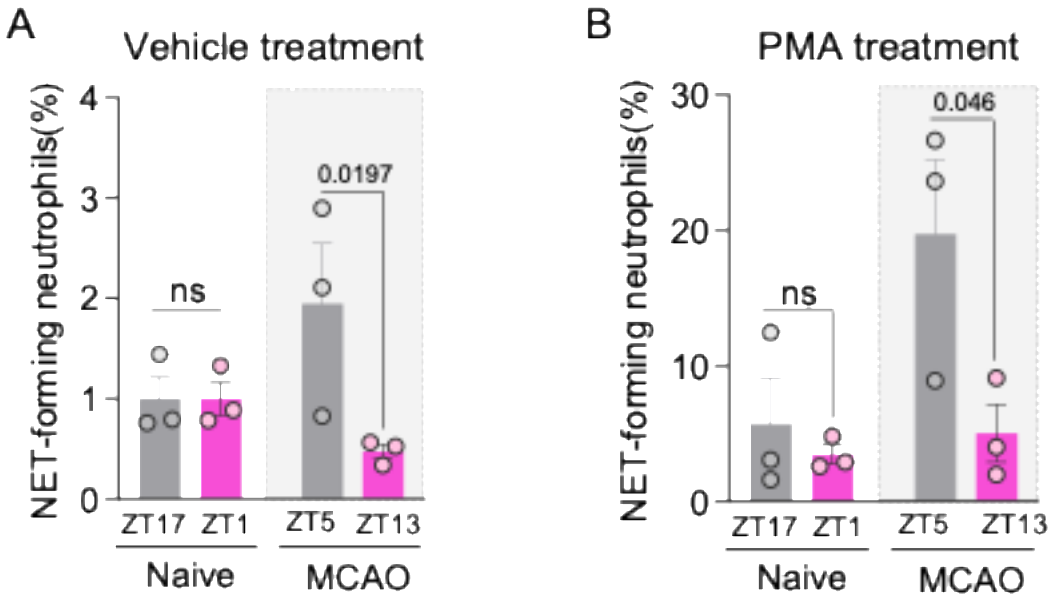

Supplementary Figure 12. NETosis as a circadian-dependent mechanism promoting microthrombosis after stroke**.** (A-B) Quantification of NET-forming neutrophils (%) in vehicle (A) and PMA treatment (B) in both naïve control group (at ZT17 and ZT1) and 12 hours after ZT5 and ZT13 MCAO group in a NETosis *ex vivo* assay. N=3 in a single experiment MCAO ZT5 and ZT13 mice. From each mouse, at least 100,000 neutrophils were isolated and divided into vehicle and PMA groups. When additional neutrophils could be isolated, duplicate samples for each condition were generated (biological replicates). Data was compared by Scheirer-Ray-Hare Test followed by Dunn/Mann-Whitney test. In (A), a significant interaction between surgery and circadian time was detected. ZT13 MCAO vehicle vs. ZT5 MCAO vehicle (*p=0.0197). In (B), a significant effect for circadian time was detected. ZT5 MCAO PMA vs. ZT13 MCAO PMA (*p=0.046). Data are shown as mean ± SEM.

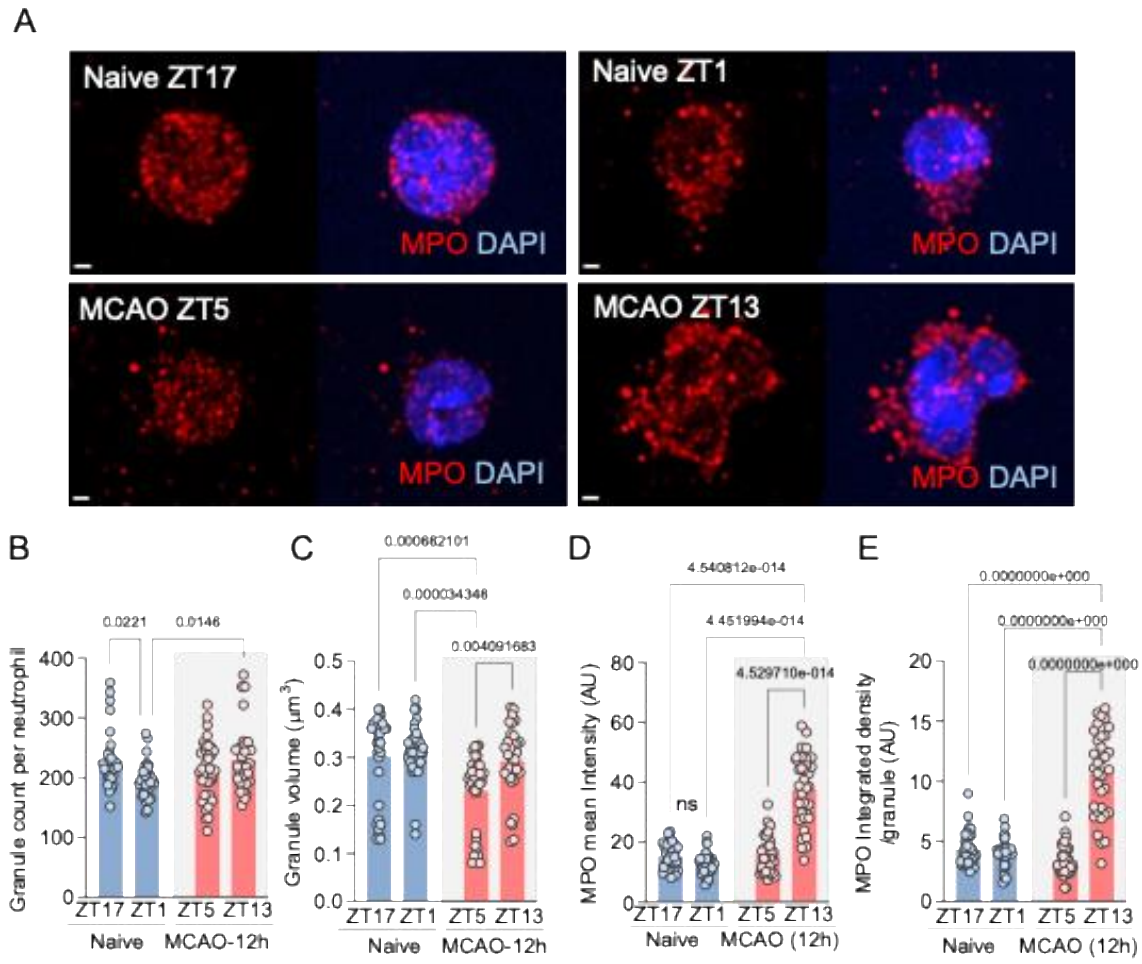

Supplementary Figure 13. Myeloperoxidase^{+} granule quantification from blood isolated neutrophils after stroke. (A) Representative immunofluorescence images of blood neutrophils from control group (ZT17 and ZT1 naïve mice in a single experiment) and 12h after MCAO group (stroke at ZT5 and ZT13 in a single experiment). MPO is in red and nuclei, stained with DAPI, are in blue. Scale bar= 5µm. (B) Quantification of the number of MPO granules per neutrophil. Naive ZT5 and ZT13 (n=32 and 33 neutrophils, respectively; 3 mice) and MCAO ZT5 and ZT13 (n=38 and 32 neutrophils, respectively; 3 MCAO mice). (C) Quantification of the mean granule volume (µm^3) per neutrophil. Naive ZT5 and ZT13 (n=32 and 34 neutrophils, respectively; 3 mice) and MCAO ZT5 and ZT13 (n=38 and 34 neutrophils, respectively; 3 MCAO mice). (D) MPO mean intensity measured as arbitrary units (AU). Naive ZT5 and ZT13 (n=32 and 34 neutrophils, respectively; 3 mice) and MCAO ZT5 and ZT13 (n=38 and 34 neutrophils, respectively; 3 MCAO mice). (E) MPO integrated density per granule (AU). Naive ZT5 and ZT13 (n=38 and 34 neutrophils, 3 mice) and MCAO ZT5 and ZT13 (n=38 and 34 neutrophils, respectively; 3 MCAO mice). A non-parametric 2-WAY ANOVA was (after normality was confirmed by the Shapiro-Wilk test). In (B), significant interaction between stroke and circadian time was found ($F(1,131)=10.6$, $p=0.0014$). Naive ZT17 vs. Naive ZT1 (*p=0.0221). In (C), significant effects were found in both stroke ($F(1,134)=8.226$, $p=0.0048$) and circadian time ($F(1,134)=13.44$, $p=0.0004$). ZT5 MCAO vs. ZT13 MCAO (*p=0.0041) and ZT17 naive vs. ZT5 MCAO (*p=0.007). In (D), a significant interaction between stroke and circadian time was found ($F(1,134)=96.50$, $P=0.0001$). ZT5 MCAO vs. ZT13 MCAO (*p<0.00001). In (E), a significant interaction between stroke and circadian time was detected $F(1,133)=111.3519$ (*<0,0001). ZT5 MCAO vs. ZT13 MCAO (*p<0.00001). Data are shown as mean ± SEM.

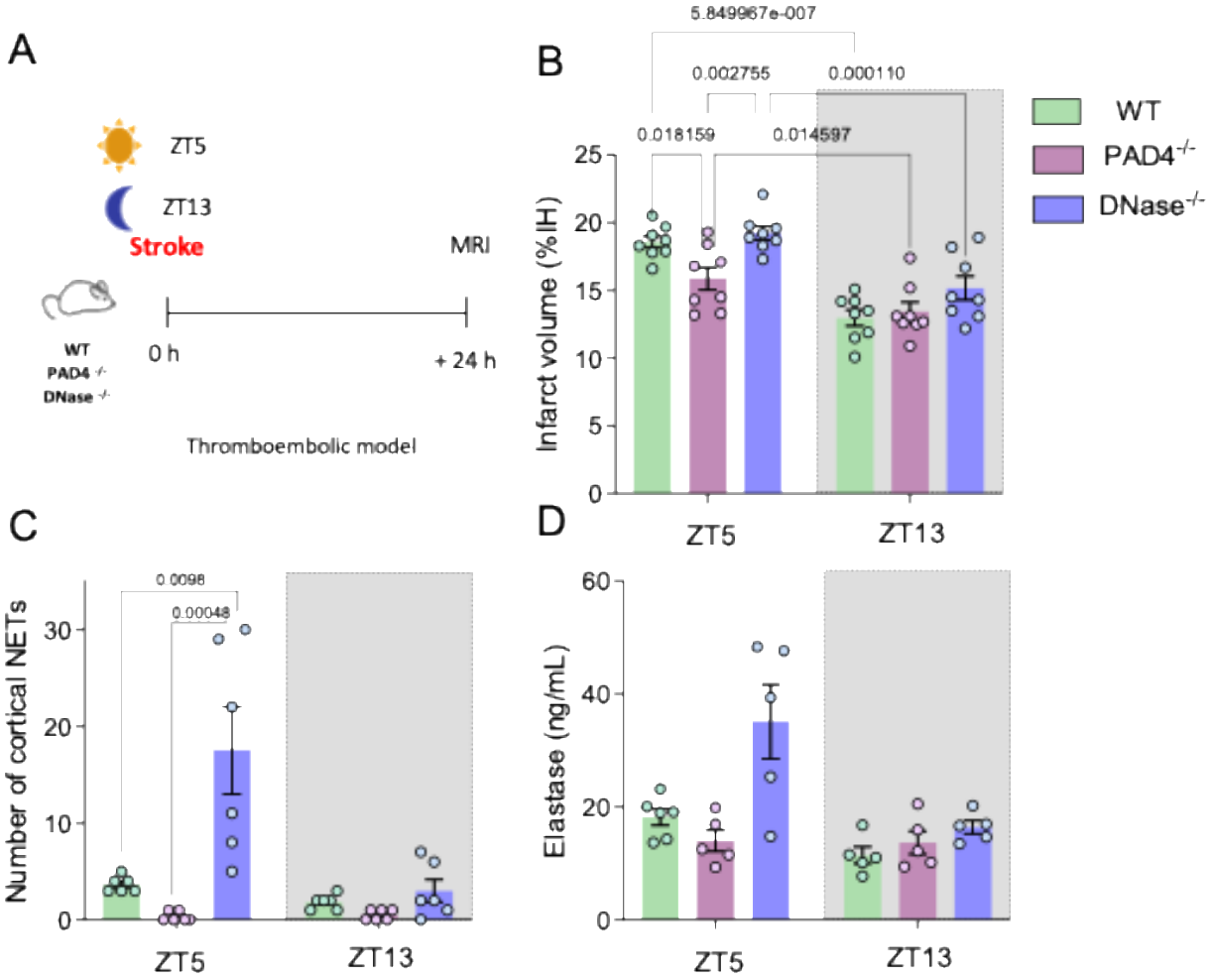

Supplementary Figure 14. Effect of the modulation of NETosis in an *in situ* thromboembolic model. (A) Quantification of the percentage of infarcted hemisphere in a *in situ* thromboembolic model at both ZT5 and ZT13 in WT, Pad4$^{-/-}$ and DNase1/3$^{-/-}$ mice (n=8 mice per group in independent experiments according to ZT). Data was compared by 2-way ANOVA followed by Tuckey post hoc (Data passed normality testing by Shapiro–Wilk test). A significant effect was detected for both the circadian time (F(1,42)=3.7509, p=4,897034x10^{-9}) and the genotype (F(2,42)=7.24625, p=0.001979). (B) Number of cortical NETs in the *in situ* thromboembolic model both at ZT5 and ZT13 in WT group, Pad4$^{-/-}$ group and DNase$^{-/-}$ group (n=8 mice per group in independent experiments according to ZT). Data was compared by non-parametric ART ANOVA followed by Emmeans post hoc. A significant effect was detected for both the genotype (F(2,30)= 23.2810, p=7.88x10^{-7}) and the circadian time (F(1,30)=18.566, p=0.00016236). A significant interaction was also observed F(2,30)=14.177, p= 4.77x10^{-5}). WT vs. DNase$^{-/-}$ ZT5 (*p=0.0098). Pad4$^{-/-}$ vs. DNase$^{-/-}$ ZT5 (*p=0.00048). (C) Elastase quantification (ng/mL) in the thromboembolic model at ZT5 and ZT13 in WT, Pad4$^{-/-}$ and DNase$^{-/-}$ groups (n=5 mice per group except for ZT5 WT, n=6). Data was compared by non-parametric ART ANOVA followed by Emmeans post hoc. A significant interaction was detected ((F(2,25)=6.250, p=0.00629081). Data are shown as mean ± SEM.

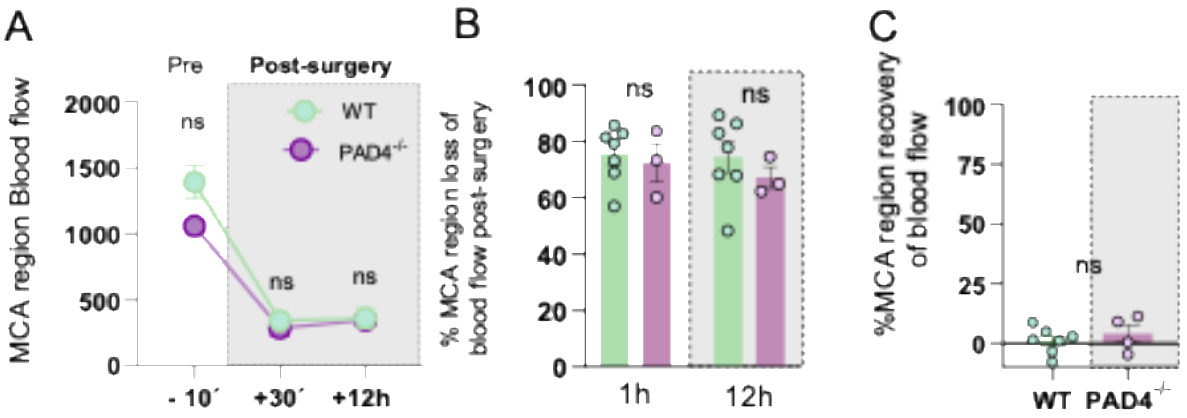

Supplementary Figure 15. Evaluation of cerebral blood flow in a NETosis deficient model caused by genetic deletion of PAD4. (A) MCA region blood flow quantification 10 minutes before stroke (-10‘), 30 minutes after stroke (+30‘) and 12 hours after stroke (+12 h) in WT and Pad4$^{-/-}$ animals at ZT5 (n=4 mice per group in a single experiment). Data was compared by non-parametric ART ANOVA followed by Emmeans post hoc. A significant effect was detected for time before/after stroke ($F(2,15)=15.1335$, $p=0.0002525$). (B) Percentage of blood flow loss in MCA region both 30 minutes and 12 hours after ischemia compared to the pre-surgery time point at ZT5 in both WT and PAD4$^{-/-}$ group. ART ANOVA analysis detected a significant effect in the genotype ($F(2,10)= 8.6719$, $p=0.015$). (C) Percentage of blood flow recovery 12 hours after ischemia (12 h) compared to the pre-surgery time point (-10’) at ZT5 in both WT and PAD4$^{-/-}$ group. No significant differences were detected by Mann Whitney test ($p=0.4857$) in (C). Data are shown as mean ± SEM.

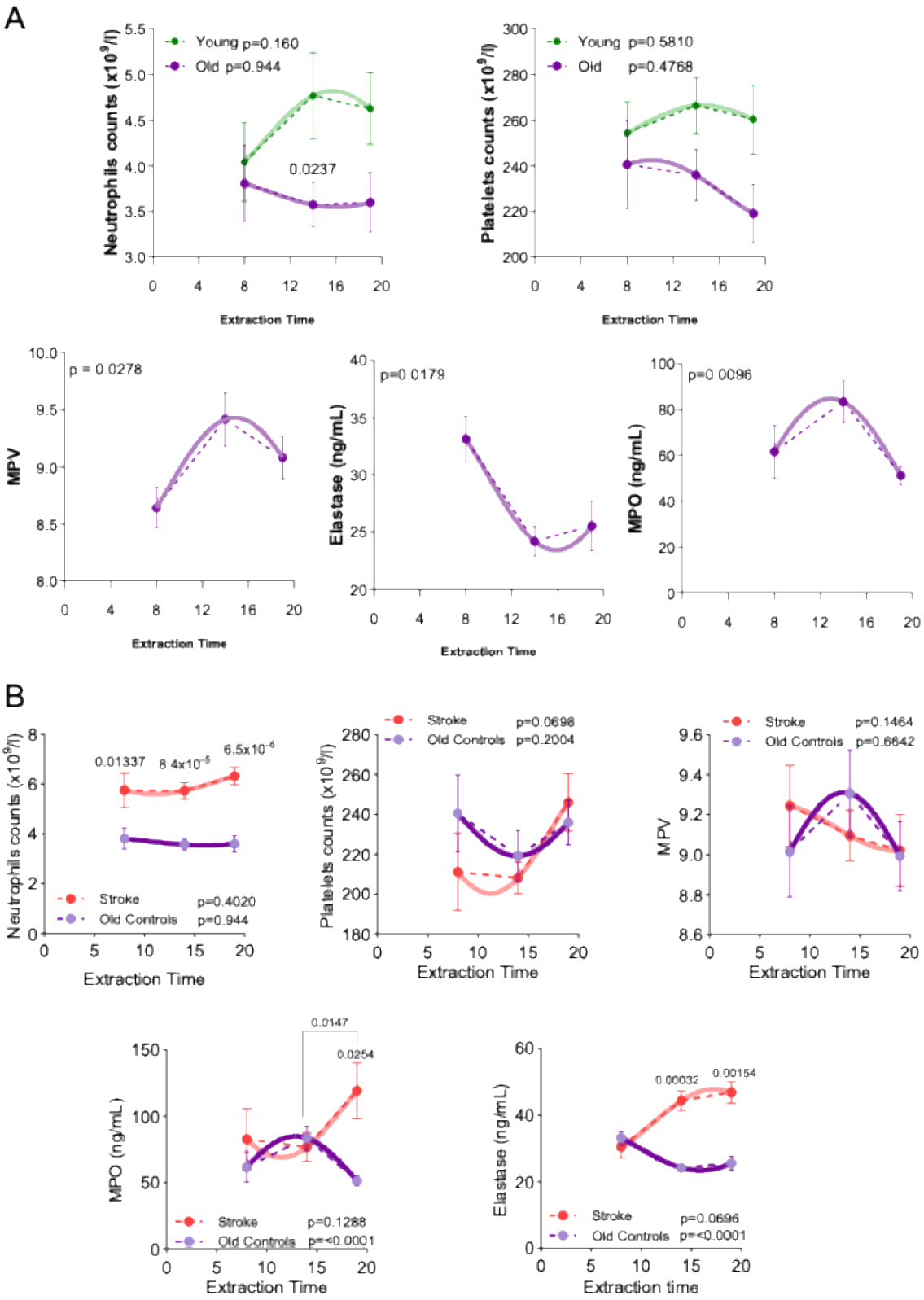

Supplementary Figure 16. Circadian analysis of blood parameters in controls and patients. (A) Circadian analysis of blood parameters in young and old healthy controls**.** Blood samples were collected from healthy individuals at three time points during the day (approximately 8:00 AM, 2:00

PM, and 7:00–8:00 PM), and the levels of various circulating parameters were analyzed in young (green; n=9, 13 and 9, respectively for each time point) and old (purple; n=13, 16 and 14, respectively for each time point) participants in each time point. Cosinor analysis was performed to assess the presence of circadian rhythmicity in each parameter. Top panels: Neutrophil and platelet counts did not show a significant circadian rhythm in either young or old individuals although a trend toward rhythmicity was more apparent in younger individuals but was absent in older subjects. Bottom panels: VPM (p=0.0278), elastase (p=0.0179), and MPO levels (p=0.0096) exhibited significant circadian rhythmicity. Comparison between neutrophil and platelet counts in young and old participants in each collection time was performed by 2-way ANOVA followed by Tuckey post hoc test (normality assessed by Shapiro Wilk Test). A significant effect was observed for the age in both neutrophils ($F(1,61)= 6.703$, $p=0.0120$) and platelets ($F(1,58)= 4.598$, $p=0.0360$). P-values for multiple comparisons are indicated in the graph. (B) Comparison of circadian patterns in stroke patients and age-matched healthy controls at equivalent sampling times. To directly compare stroke patients and healthy controls at matched time points, a subcohort of stroke patients (n=366) with known stroke onset times was used to select samples drawn at approximately 8:00 AM, 2:00 PM, and 7:00–8:00 PM, corresponding to the time points used for healthy controls. This yielded 9, 59, and 34 patients per time window, respectively. The red curves represent stroke patients, and the purple curves represent old healthy controls. Cosinor analysis was performed to assess rhythmicity, with corresponding p-values shown for each parameter. Data was analyzed by ART ANOVA followed by multiple Mann–Whitney U tests (Holm–Šídák correction). Significant effects for stroke condition were detected for neutrophil counts ($F(1,139)=45.449$, $p=3.854\times10^{-10}$. P-values for multiple comparisons are indicated in the graph. A significant interaction between stroke condition and collection time was detected for MPO levels ($F(2,149)= 5.231$, $p=0.00637$) and elastase levels ($F(2,115)= 3.196$, $p=0.0445$). Post hoc comparisons for MPO: Controls 19-20h vs. Stroke 19-20h (*p=0.0254) and Stroke 13-14h vs. Stroke 19-20h (*p=0.0147). Post hoc comparisons for Elastase: Controls 13-14h vs. Stroke 13-14h (*p=0.000319) and Controls 19-20h vs. Stroke 19-20h (*p=0.0154). Data are shown as mean ± SEM.

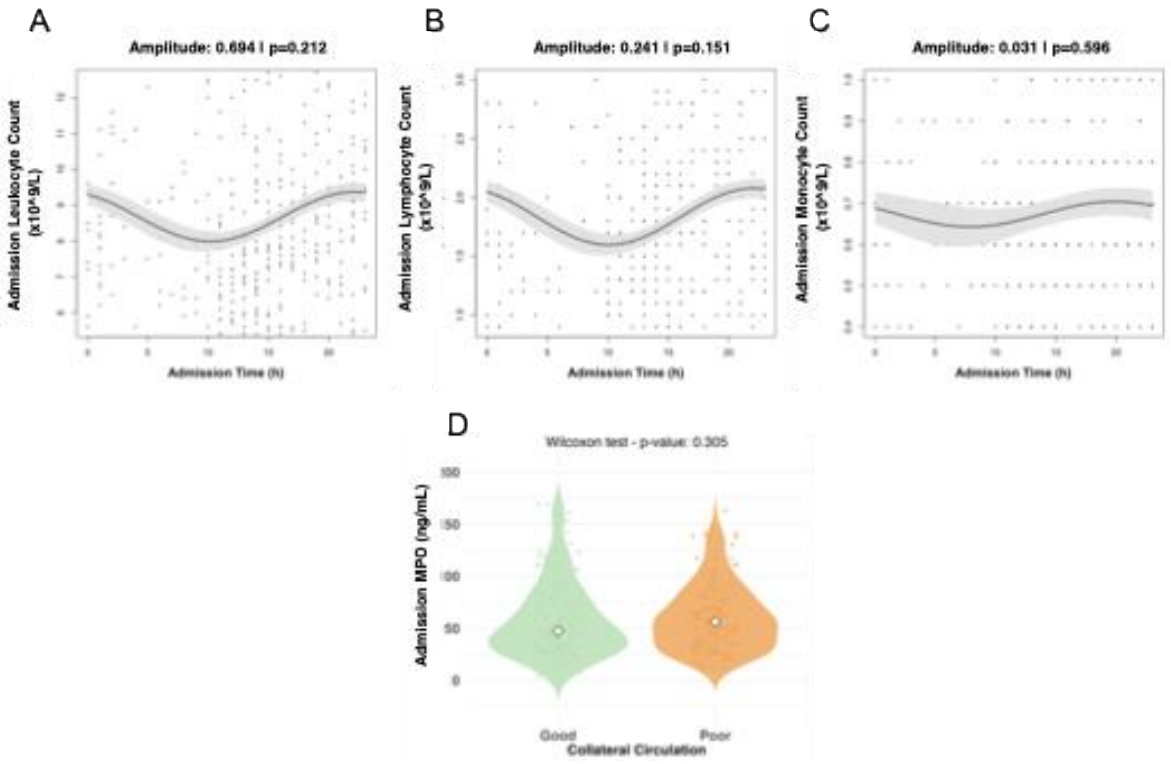

Supplementary Figure 17. Stroke patients display diurnal oscillations in stroke severity, immunothrombosis and NETosis markers linked to collateral circulation. (A-C) Diurnal oscillations of admission hematological parameters including leukocytes, lymphocytes and monocytes. Each plot presents the COSINOR-fitted curve with a shaded ribbon representing the standard error (SE) of the fit. The amplitude and p-value of each oscillation are indicated in the plot titles; rhythms with p-values below 0.05 are considered to have significant diurnal patterns. (D) Comparative analysis of clinical markers by collateral circulation status using violin plots. Violin plots illustrate the distribution of MPO in patients with good versus poor collateral circulation (n= 349). Violin plot includes data points (jittered) and displays the median as a white diamond. Outliers were removed using the interquartile range (IQR) method, with outliers defined as values lying beyond 1.5 times the IQR from the first and third quartiles. For each marker, appropriate statistical tests were conducted based on data distribution. t-test applied to admission elastase and Wilcoxon tests applied to admission NIHSS and infarct size.

Online Tables S1-S9

FOOTPRINT (parameter)		ZT5 Baseline		ZT5 MCAO		ZT13 Baseline		ZT13 MCAO	
		MEAN	SD	MEAN	SD	MEAN	SD	MEAN	SD
Hindlimb stride length (cm)	Contralateral (right)	6.938	0.211	6.821	0.720	6.983	0.914	7.024	0.807
	Ipsilateral (left)	7.056	0.328	6.893	0.792	6.905	0.638	6.996	0.803
Sway width (cm)	Forelimb	1.641	0.235	1.862	0.138	1.607	0.173	1.577	0.147
	Hindlimb	2.619	0.415	2.659	0.136	2.651	0.136	2.369	0.147
Overlap (average forelimb and hindlimb; cm)		0.762	0.370	0.726	0.359	0.659	0.255	0.527	0.304

Supplementary Table S1. Evaluation of motor impairment after stroke by footprint test. Main parameters measured in the footprint test: hindlimb stride length (cm), sway width (cm) and overlap (average forelimb and hindlimb; cm). All these parameters were measured in ZT5 and ZT13 mice during the baseline (48h before stroke) and 24h after stroke.

Supplementary Table S2. Enriched pathways in differentially expressed genes from each cluster

Supplementary Table S3. Differentially expressed genes in WT Brain at ZT13 vs. ZT5 per cluster

Supplementary Table S4. Enriched pathways in differentially expressed genes in WT Brain at ZT13 vs. ZT5 per cluster

	Overall
n	**366**
Age, mean (SD)	76.00 [63.25, 84.00]
Gender (Female), n (%)	187 (51.1)
Previous mRS, n (%)	
mRS 0	283 (77.1)
mRS 1	51 (13.9)
mRS 2	33 (9.0)
Tobacco, n (%)	
Non smoker	246 (68.3)
Active smoker	64 (17.8)
Past smoker	50 (13.9)
Alcohol, n (%)	
Non Alcohol Use	310 (87.1)
Alcohol Use	34 (9.6)
Past Alcohol Use	12 (3.4)
Hypertension, n (%)	250 (68.3)
Dyslipidemia, n (%)	216 (59.0)
Diabetes, n (%)	95 (26.0)
Atrial Fibrillation, n (%)	96 (26.2)
Metallic Valve, n (%)	14 (3.8)
Previous Ischemic Stroke, n (%)	55 (15.0)
Previous Hematoma, n (%)	5 (1.4)
Previous Myocardial Infarction, n (%)	37 (10.1)
Arteriopathy, n (%)	27 (7.4)
Chronic Kidney Disease, n (%)	22 (6.0)
Previous Antihypertensive Therapy, n (%)	230 (62.8)
Previous Lipid-Lowering Therapy, n (%)	189 (51.6)
Previous Antiplatelet Therapy, n (%)	88 (24.0)
Previous Anticoagulant Therapy, n (%)	84 (23.0)

Supplementary Table S5. Baseline characteristics of ischemic stroke cohort with known onset (n=366). Results are presented as median [IQR] or count (%).

	Overall
n	37
Age, mean (SD)	68.43 (8.19)
Gender (Female), n (%)	26 (70.3)
Tobacco, n (%)	
– Non-smoker	15 (40.5)
– Active smoker	6 (16.2)
– Past smoker	16 (43.2)
Hypertension, n (%)	36 (97.3)
Dyslipidemia, n (%)	13 (35.1)
Diabetes, n (%)	4 (10.8)
Atrial Fibrillation, n (%)	4 (10.8)
Antiplatelet Therapy, n (%)	13 (35.1)
Anticoagulant Therapy, n (%)	9 (25.4)

Supplementary Table 6. Demographic and clinical characteristics of the matched-age ("old") control group. Summary of demographic and vascular risk factors in 37 non-stroke control individuals used for comparative analyses. Data are expressed as mean ± SD for continuous variables and as number and percentage for categorical variables.

	Overall
n	366
Stroke Onset-to-Hospital Time, mean (SD)	2.00 [1.00, 4.00]
Admission Blood Glucose, mean (SD)	118.00 [103.00, 142.25]
Admission Leukocytes, mean (SD)	8.10 [6.80, 9.88]
Admission Neutrophils, mean (SD)	5.50 [4.10, 7.00]
Admission Lymphocytes, mean (SD)	1.70 [1.20, 2.30]
Admission Monocytes, mean (SD)	0.60 [0.50, 0.80]
Admission Platelets, mean (SD)	211.00 [171.00, 261.00]
Admission MPV, mean (SD)	9.00 [8.30, 9.70]
Admission Neutrophil-Specific Elastase, mea	37.93 [27.43, 56.80]
Admission Myeloperoxidase, mean (SD)	57.30 [36.12, 89.21]
Admission sCD40L, mean (SD)	0.30 [0.15, 0.55]
Admission NIHSS, mean (SD)	10.00 [4.00, 18.00]
Infarct Volume (cc), mean (SD)	3.58 [0.25, 18.88]
Poor Collateral Circulation, mean (SD)	129 (56.6)
Etiology	
Atherothrombotic	116 (31.9)
Cardioembolic	141 (38.7)
Cryptogenic	28 (7.7)
Coexistence of Cause	31 (8.5)
Incomplete Study	28 (7.7)
Unusual Cause	20 (5.5)
tPA, n (%)	163 (46.0)
Thrombectomy, n (%)	214 (59.9)
Post-hemorrhage, n (%)	56 (16.5)
NIHSS at Stroke Unit, mean (SD)	3.00 [1.00, 9.00]
mRS 3 months	
Independent	219 (63.8)
Dependent	83 (24.2)
All-cause mortality	41 (12.0)

Supplementary Table S7. Clinical characteristics, therapeutic management, and prognostic indicators of the ischemic stroke cohort (n=366). Results are presented as median [IQR] or count (%).

Biomarker	MESOR ± SE	Amplitude ± SE	Amplitude p-value	Acrophase (hours) ± SE	rophase p-va	ak max (valu	Peak max (h)
Cosinor model fitted based on time of admission							
Admission Leukocytes	8.678 ± 0.167	0.694 ± 0.204	**0.001**	22.169 ± 1.360	0.183	9,296	22
Admission Neutrophils	5.984 ± 0.163	0.402 ± 0.199	**0.043**	22.281 ± 2.299	0.455	6,346	22
Admission Lymphocytes	1.838 ± 0.053	0.241 ± 0.066	**0.000**	22.067 ± 1.249	0.122	2,049	22
Admission Platelets	216.786 ± 4.340	15.681 ± 5.573	**0.005**	21.414 ± 1.509	0.087	231,011	21
Admission Mean Platelet Volume	9.047 ± 0.065	0.178 ± 0.078	**0.022**	12.661 ± 2.053	0.736	9,222	13
Admission sCD40L	0.427 ± 0.028	0.089 ± 0.036	**0.014**	21.086 ± 1.650	0.088	0,493	21
Admission log Neutrophil-Elastase	3.678 ± 0.036	0.096 ± 0.055	0.079	17.619 ± 1.692	**0.001**	3,668	18
Admission log Myeloperoxidase	3.995 ± 0.046	0.200 ± 0.071	**0.005**	18.977 ± 1.104	**0.000**	4,046	19
Cosinor model fitted based on time of symptom onset							
Admission NIHSS	11.480 ± 0.493	1.534 ± 0.591	**0.009**	20.020 ± 1.841	**0.031**	12,253	20
24h post-stroke NIHSS	5.946 ± 0.432	1.159 ± 0.619	0.063	5.649 ± 1.830	**0.002**	6,051	6
Delta NIHSS (24-admission)	42.356 ± 4.454	9.391 ± 6.517	0.150	13.547 ± 2.235	0.489	50,988	14
Infarct Volume (cc)	24.294 ± 3.887	12.928 ± 5.957	**0.030**	16.358 ± 1.345	**0.001**	29,674	16

Supplementary Table S8. Table showing diurnal patterns of blood markers at admission and clinical variables in acute stroke patients after COSINOR adjustment. The table shows the diurnally adjusted estimates (Estimate ± Standard Error) of blood markers at admission and clinical variables in acute stroke patients. Each variable includes MESOR, amplitude, acrophase (in hours), and the corresponding p-value, providing insights into the timing and intensity of diurnal patterns.

	Group	Initial N (animals/samples)	Removed (n)	Reason for exclusion	Final N
Fig. 1B	ZT19	20	1	Striatal infarction detected on TTC	19
Fig. 1G	ZT13	12	1	Hemorrhage detected on MRI	11
Fig. 1H	ZT5 baseline	5	1	Incomplete behavioral assessment	4
	ZT13 baseline	5	1	Incomplete behavioral assessment	4
Supp. Fig. 1H	ZT1	5	1	Technical error during sample processing	4
	ZT9	5	1	Technical error during sample processing	4
	ZT21	4	1	Technical error during sample processing	3
Supp. Fig. 1I	ZT1	5	1	Technical error during sample processing	4
	ZT5	5	1	Outlier value from group mean	4
	ZT13	5	1	Technical error during sample processing	4
Fig. 2C	ZT13 isotype	10	2	Striatal infarction detected on TTC	8
Fig. 2F	ZT5 WT	12	1	Hemorrhage detected on MRI	11
	ZT13 WT	10	1	Striatal infarction detected on MRI	9
	ZT5 $CXCR4^{Neu}$	4	1	Outlier value from group mean	3
Fig. 2I	AMD	8	2	Technical error during MRI	6
	$BMAL^{Neu}$	5	1	Technical error during MRI	4
Supp. Fig. 3C	AMD	8	2	Technical error during MRI	6
	$BMAL^{Neu}$	5	1	Technical error during MRI	4
Fig. 3 B	ZT5 24h	9	1	Outlier value from group mean	8
Supp. Fig. 4B	ZT13 pMCAO	7	1	Outlier value from group mean	6
Supp. Fig. 4D	ZT13 12h	7	1	Outlier value from group mean	6
Supp. Fig. 5B	ZT5	22	1	Outlier value from group mean	21
Supp. Fig. 12B	ZT1 control	34	1	Outlier value from group mean	33
Supp. Fig. 15 A-B-C	$PAD4^{-/-}$	4	1	Technical error during blood flow measurement	3
Supp. Fig. 16 A	Elastase levels	31	2	Outlier values from group mean	29
	MPO levels	31	2	Outlier values from group mean	29

Supplementary Table S9. Description of removed outliers and excluded samples/animals.

Major Resources Table

In order to allow validation and replication of experiments, all essential research materials listed in the Methods should be included in the Major Resources Table below. Authors are encouraged to use public repositories for protocols, data, code, and other materials and provide persistent identifiers and/or links to repositories when available. Authors may add or delete rows as needed.

Animals (in vivo studies)

Species	Vendor or Source	Background Strain	Sex	Persistent ID / URL
Mus musculus	Mice (C57BL/6OlaHsd) were originally obtained from Envigo and provided to us by CNIC	C57BL/6OlaHsd	Male	RRID:IMSR_HAR:162
Mus musculus	The Jackson Laboratory	PAD4$^{-/-}$	Male	RRID:IMSR_JAX:030315
Mus musculus	Supply by Hidalgo's lab	Bmal$^{fl/fl}$MRP8^{Cre} or Bmal1^{Neu}	Male	N/A (internal colony)
Mus musculus	Supply by Hidalgo's lab	Cxcr4$^{fl/fl}$MRP8^{Cre} or Cxcr4^{Neu}	Male	N/A (internal colony)
Mus musculus	Supply by Hidalgo's lab	Ly6G^{tdTom}	Male	N/A (internal colony)
Mus musculus	Supply by Napirei's lab	D1$^{-/-}$D1l3$^{-/-}$ or DNase$^{-/-}$	Male	N/A (internal colony)

Genetically Modified Animals

	Species	Vendor or Source	Background Strain	Other Information	Persistent ID / URL
Parent - Male	Mus musculus	The Jackson Laboratory	**BMAL$^{f/f}$** B6.129S4(Cg)-Bmal1tm1Weit/J	Floxed BMAL1 allele	RRID:IMSR_JAX:007668
Parent - Male	Mus musculus	The Jackson Laboratory	**CXCR4$^{f/f}$** B6.129P2-Cxcr4tm2Yzo/J	Floxed CXCR4 allele	RRID:IMSR_JAX:008767
Parent - Female	Mus musculus	The Jackson Laboratory	**MRP8^{cre}** B6.Cg-Tg(S100A8-cre,-EGFP)1Ilw/J	Neutrophil-specific Cre driver	RRID:IMSR_JAX:021614

DOI [to be added]

Parent - Male	Mus musculus	The Jackson Laboratory	PAD4$^{-/-}$	Lack exons 9-10 of the peptidyl arginine deiminase type IV (Padi4) gene	RRID:IMSR_JAX:030315
Parent - Female	Mus musculus	Supply by Hidalgo's lab	Ly6G^{tdTom}	High levels of tdTomato fluorescence in neutrophils	N/A (internal colony)
Parent - Female	Mus musculus	Supply by Napirei's lab	Dnase1$^{-/-}$	Lack functional deoxyribonuclease 1 (Dnase1)	N/A (internal colony)
Parent - Female	Mus musculus	Supply by Napirei's lab	Dnase1l3$^{-/-}$	Lack functional deoxyribonuclease 1-like 3 (Dnase1l3)	N/A (internal colony)

Antibodies

Target antigen	Vendor or Source	Catalog #	Working concentration	Persistent ID / URL
Ly6G	BD Biosciences	551461	1: 1000	AB_394208
CD45	BD Biosciences	553080	1: 1000	AB_394609
CD11b	BD Biosciences	101263	1: 1000	AB_2629529
CD182 (CXCR2)	BD Biosciences	149308	1: 1000	AB_396229
CD184 (CXCR4)	BD Biosciences	146508	1: 1000	AB_2562785
CD62L	BD Biosciences	104405	1: 1000	AB_313092
Ly-6C	BD Biosciences	128005	1: 1000	AB_1186134
Human/Mouse Myeloperoxidase/MPO	R&D Systems	AF3667	1: 200	AB_2250866
Histone H3 (citrulline R2 + R8 + R17)	Abcam	ab5103	1: 400	AB_304752
H3 3D9 Cleaved Histone CLIPPING	Supply by Arturo Zychlinsky's lab	N/A	1: 200	https://pmc.ncbi.nlm.nih.gov/articles/PMC9665850/
Pan Laminin	Novus Biologicals	NB300-144B	1: 250	AB_10001146
CD41	Bioscience	553847	1: 200	AB_395084
Alexa Fluor 647 Anti-Rabbit	Thermo Fisher Scientific	A-21443	1:500	N/A
Donkey anti Goat IgG (H+L) Secondary Antibody, Biotin, Invitrogen	Thermo Fisher Scientific	A16003	1: 200	AB_2534677
Chicken anti-rat *Alexa Fluor* 647	Invitrogen	A21472	1: 500	N/A

Streptavidin, Alexa Fluor™ 488 conjugate	Thermo Fisher Scientific	S32354	1: 500	N/A
Streptavidin, Alexa Fluor™ 405 conjugate	Thermo Fisher Scientific	S32351	1: 500	N/A
Lectin (LEL, TL) 488	Vector Laboratories	FL-1171	1: 100	N/A

Data & Code Availability

Description	Source / Repository	Persistent ID / URL
Single-cell RNA-seq raw and processed data from brain-infiltrating neutrophils after ischemic stroke (mouse model)	GEO (NCBI Gene Expression Omnibus)	GSE290318

DOI [to be added]

ARRIVE GUIDELINES

The ARRIVE guidelines (https://arriveguidelines.org/) are a checklist of recommendations to improve the reporting of research involving animals. Key elements of the study design should be included below to better enable readers to scrutinize the research adequately, evaluate its methodological rigor, and reproduce the methods or findings.

Study Design

Groups	Sex	Age	Number (prior to experiment)	Number (after termination)	Litterm ates (Yes / No)	Other description
Group 1 ZT1 WT; ZT5 WT; ZT13 WT; ZT19 WT	Male	3 months	ZT1 WT: 10; ZT5 WT: 10; ZT13 WT:10; ZT19 WT:10	ZT1 WT: 19 ZT5 WT: 20 ZT13 WT:20 ZT19 WT:19	No	Infarct volume determination based on activity in distal ischemia models
Group 2 ZT5 WT; ZT13 WT	Male	15 months (aged cohort)	ZT5 WT: 5; ZT13 WT: 5	ZT5 WT: 5 ZT13 WT: 5	No	Infarct volume determination based on activity in old animals
Group 3 ZT5 WT; ZT13 WT	Male	3 months	ZT5 WT: 5; ZT13 WT: 5	ZT5 WT: 5 ZT13 WT: 4	No	Assessment of neurological deficits by the footprint test
Group 4 Naïve WT	Male	3 months	Naïve WT: 8	Naïve WT: 8	No	Circadian rhythmicity of metabolic and behavioural parameters in wild-type Naive mice
Group 5 ZT1 WT Naive; ZT5 WT Naive; ZT9 WT Naive; ZT13 WT Naive; ZT17 WT Naive; ZT21 WT Naive	Male	3 months	ZT1 WT Naïve:8 ; ZT5 WT Naïve: 8; ZT9 WT Naïve: 8; ZT13 WT Naïve: 8; ZT17 WT Naïve: 8; ZT21 WT Naïve: 8	ZT1 WT Naïve: 4 ZT5 WT Naïve: 5 ZT9 WT Naïve: 4 ZT13 WT Naïve: 5 ZT17 WT Naïve: 5 ZT21 WT Naïve: 3	No	Circadian rhythmicity of melatonin, corticosterone and time-dependent variation in leukocyte populations in peripheral blood in wild-type Naive mice
Group 6 Isotype ZT5 WT; anti-Ly6G ZT5 WT; isotype ZT13 WT; anti-Ly6G ZT13 WT	Male	3 months	Isotype ZT5 WT: 8; anti-Ly6G ZT5 WT: 8; isotype ZT13 WT: 8; anti-Ly6G ZT13 WT: 8	Isotype ZT5 WT: 7 anti-Ly6G ZT5 WT: 8 isotype ZT13 WT: 8 anti-Ly6G ZT13 WT: 9	No	Infarct volume determination and quantification of neutrophils in blood after the administration of anti-Ly6G

						antibody ZT5 vs ZT13
Group 7 ZT5 WT; ZT13 WT; ZT5 $Bmal^{neu}$; ZT13 $Bmal^{neu}$; ZT5 $Cxcr4^{neu}$; ZT13 $Cxcr4^{neu}$	Male	3 months	ZT5 WT: 6; ZT13 WT: 6; ZT5 $Bmal^{neu}$: 6; ZT13 $Bmal^{neu}$: 6; ZT5 $Cxcr4^{neu}$: 6; ZT13 $Cxcr4^{neu}$: 6	ZT5 WT: 8 ZT13 WT: 10 ZT5 $Bmal^{neu}$: 4 ZT13 $Bmal^{neu}$: 6 ZT5 $Cxcr4^{neu}$: 3 ZT13 $Cxcr4^{neu}$: 3	No	Infarct volume determination and quantification of the total number of neutrophils in brain ZT5 vs ZT13
Group 8 WT saline donors to $Ly6G^{tdTom}$ recipient animals; $Bmal^{fl/fl}MRP8^{Cre-}$ donors to $Ly6G^{tdTom}$ recipient animals; $Bmal^{fl/fl}MRP8^{Cre+}$ donors to $Ly6G^{tdTom}$ recipient animals	Male	3 months	WT saline donors to $Ly6G^{tdTom}$ recipient animals: 6; $Bmal^{fl/fl}MRP8^{Cre-}$ donors to $Ly6G^{tdTom}$ recipient animals: 6; $Bmal^{fl/fl}MRP8^{Cre+}$ donors to $Ly6G^{tdTom}$ recipient animals: 6	WT saline donors to $Ly6G^{tdTom}$ recipient animals: 5; $Bmal^{fl/fl}MRP8^{Cre-}$ donors to $Ly6G^{tdTom}$ recipient animals: 6; $Bmal^{fl/fl}MRP8^{Cre+}$ donors to $Ly6G^{tdTom}$ recipient animals: 4	Yes	Infarct volume determination and quantification of transferred blood neutrophils/ml, transferred brain neutrophils and transferred neutrophils density from donors in receptor animals
Group 9 ZT5 $Ly6G^{tdTom}$; ZT13 $Ly6G^{tdTom}$	Male	3 months	ZT5 $Ly6G^{tdTom}$:10; ZT13 $Ly6G^{tdTom}$:10	ZT5 $Ly6G^{tdTom}$:63 ZT13 $Ly6G^{tdTom}$:70	No	Neutrophil quantification and localization studies in brain at 5h, 12 h, and 24 h after ischemia ZT5 vs ZT13. Plasma elastase levels measurement.
Group 10 ZT5 WT; ZT13 WT	Male	3 months	ZT5 WT: 3; ZT13 WT: 3	ZT5 WT: 3; ZT13 WT: 3	No	Blood perfusion assessment by laser speckle 10min before ischemia and 30min and 12h after ischemia ZT5 vs ZT13
Group 11 ZT5 $Ly6G^{tdTom}$; ZT13 $Ly6G^{tdTom}$	Male	3 months	ZT5 $Ly6G^{tdTom}$:10; ZT13 $Ly6G^{tdTom}$;10	ZT5 $Ly6G^{tdTom}$:10; ZT13 $Ly6G^{tdTom}$:10	No	scRNA-sequencing of sorted brain neutrophils 12h after ischemia ZT5 vs ZT13
Group 12	Male	3 months	ZT5 WT: 3; ZT5 WT Naïve:3; ZT13 WT: 3;	ZT5 WT: 3 ZT5 WT Naïve: 3 ZT13 WT: 3	No	*Ex vivo* NETosis assays of blood-

ZT5 WT; ZT5 WT Naive; ZT13 WT; ZT13 WT Naive			ZT13 WT Naïve: 3	ZT13 WT Naïve: 3		isolated neutrophils
Group 13 ZT5 Ly6G^{tdTom}; ZT13 Ly6G^{tdTom}	Male	3 months	ZT5 Ly6G^{tdTom}:3; ZT13 Ly6G^{tdTom}: 3	ZT5 Ly6G^{tdTom}:3; ZT13 Ly6G^{tdTom}: 3	No	Quantification of ischemic brain NETosis and neutrophil granule morphology (blood-isolated)
Group14 ZT5 WT treated with Cl-Amidine; ZT5 WT treated with vehicle; ZT13 WT treated with Cl-Amidine; ZT13 WT treated with vehicle	Male	3 months	ZT5 WT Cl-Amidine; ZT5 WT vehicle; ZT13 WT Cl-Amidine; ZT13 WT vehicle	ZT5 WT Cl-Amidine: 4; ZT5 WT vehicle:5; ZT13 WT Cl-Amidine: 4; ZT13 WT vehicle: 4	No	Infarct volume determination 24h after stroke ZT5 vs ZT13
Group15 ZT5 PAD4$^{+/+}$; ZT5 PAD4$^{-/-}$; ZT13 PAD4$^{+/+}$; ZT13 PAD4$^{-/-}$;	Male	3 months	ZT5 WT: 10; ZT5 PAD4$^{-/-}$: 10; ZT13 WT: 10; ZT13 PAD4$^{-/-}$: 10	ZT5 WT: 18 ZT5 PAD4$^{-/-}$: 10 ZT13 WT: 15 ZT13 PAD4$^{-/-}$: 10	No	Infarct volume determination 24h after stroke ZT5 vs ZT13
Group16 ZT5 WT; ZT5 PAD4$^{-/-}$; ZT13 WT; ZT13 PAD4$^{-/-}$;	Male	3 months	ZT5 WT: 4; ZT5 PAD4$^{-/-}$: 4; ZT13 WT: 4; ZT13 PAD4$^{-/-}$: 4	ZT5 WT: 4; ZT5 PAD4$^{-/-}$: 4; ZT13 WT: 4; ZT13 PAD4$^{-/-}$: 4	No	Blood perfusion assessment by laser speckle 10min before ischemia and 30min and 12h after ischemia ZT5 vs ZT13
Group17 ZT5 WT; ZT5 PAD4$^{-/-}$; ZT5 DNase$^{-/-}$; ZT13 WT; ZT13 PAD4$^{-/-}$; ZT13 DNase$^{-/-}$	Male	3 months	ZT5 WT: 8; ZT5 PAD4-/-: 8; ZT5 DNase-/-: 8; ZT13 WT: 8; ZT13 PAD4-/-: 8; ZT13 DNase-/-: 8	ZT5 WT: 8 ZT5 PAD4-/-: 8 ZT5 DNase-/-: 8 ZT13 WT: 8 ZT13 PAD4-/-: 8 ZT13 DNase-/-:8	No	Infarct volume determination after stroke ZT5 vs ZT13, quantification of ischemic brain NETosis and plasma elastase levels measurement.
Group18 ZT5 WT treated with DNase1; ZT5 WT treated with vehicle	Male	3 months	ZT5 WT DNase1: 5; ZT5 WT vehicle: 5	ZT5 WT DNase1: 5; ZT5 WT vehicle: 5	No	Infarct volume determination 24h after stroke

Sample Size: Please explain how the sample size was decided Please provide details of any a *prior* sample size calculation, if done.

The estimated sample size for each experimental group was calculated using the function pwrss.np.2groups () from the {pwrss} package in R 3.5.2. This function provides an estimated n based on the desired statistical power (β=80%), significance level (α=0.05), expected means and standard deviations of the populations, and kappa (the

ratio between the sample sizes of the two populations). To obtain estimates of means and standard deviations, we relied on our previous experience with similar techniques and assessments, including experimental designs in the field of mouse models of ischemic stroke, as well as data from previously published literature. This ensured that the calculated sample sizes were both statistically robust and biologically meaningful. All statistical analyses were performed by researchers blinded to the experimental conditions, further ensuring the rigor and objectivity of our results.

Inclusion Criteria and exclusión criteria

Animals that successfully underwent ischemia induction at the designated circadian times and produced technically valid behavioral, imaging, or biological data. Mice were excluded from endpoint analyses if they exhibited signs of procedure-related complications (e.g., vagus nerve impairment, spontaneous death, or striatal lesions likely due to arterial occlusion), showed no infarct at 24h after MCAO, experienced technical errors during sample processing or imaging, , or were identified as statistical outliers. In such cases, animals were euthanized and/or excluded from all experiments. Additionally, some animals or samples were excluded based on predefined outlier criteria, including Grubb's method ($\alpha = 0.05$ for a single extreme value), ROUT (Q = 1%), or interquartile range (IQR) (values < or > 1.5 IQR, applied only when n=3–5). Animals successfully undergoing ischemia induction at the designated circadian times and producing technically valid behavioral, imaging, or biological data were included. Details are provided in Supplementary Figure S9

Randomization

Animals were randomly assigned to different experimental groups, including distinct Zeitgeber times or pharmacological treatments (e.g., LY6G antibody or Cl-amidine). Randomisation sequences were generated using a computer-based random number generator to ensure unbiased allocation. To minimise potential confounders, such as treatment order or cage effects, animals were temporarily separated from untreated cage mates immediately after receiving their assigned treatment. This procedure reduced the likelihood of cross-interference or behavioral influences between treated and untreated animals.

Blinding

Analyses of histology, immunofluorescence, MRI, LSCI, behavioral outcomes, and flow cytometry were performed on coded samples or data sets by investigators blinded to group allocation. Biochemical assays were processed with coded samples, and statistical analyses were conducted without knowledge of group identity. While surgical procedures could not be performed in a blinded manner due to logistical and timing requirements, all post-surgical treatments and assessments were carried out by investigators blinded to group assignment. This approach ensured that treatment administration and subsequent data collection were unbiased.

DOI [to be added]

DOI [to be added]